

A TRANSITION STATE PHYSICOCHEMICAL MODEL PREDICTING
NITRIFICATION RATES IN SOIL-WATER SYSTEMS

by

Marvin James Shaffer

A Dissertation Submitted to the Faculty of the
DEPARTMENT OF HYDROLOGY AND WATER RESOURCES
In Partial Fulfillment of the Requirements
for the Degree of

DOCTOR OF PHILOSOPHY
WITH A MAJOR IN HYDROLOGY

In the Graduate College
THE UNIVERSITY OF ARIZONA

1 9 7 2

THE UNIVERSITY OF ARIZONA
GRADUATE COLLEGE

I hereby recommend that this dissertation prepared under my
direction by MARVIN JAMES SHAFFER
entitled A TRANSITION STATE PHYSICOCHEMICAL MODEL
PREDICTING NITRIFICATION RATES IN
SOIL-WATER SYSTEMS
be accepted as fulfilling the dissertation requirement of the
degree of DOCTOR OF PHILOSOPHY


Dissertation Director

8-30-72
Date

After inspection of the final copy of the dissertation, the
following members of the Final Examination Committee concur in
its approval and recommend its acceptance:*

<u>Samuel D. Evans</u>	<u>8/31/72</u>
<u>Heinrich L. Boh</u>	<u>31 Aug 72</u>
<u>Wallace H. Jancecs</u>	<u>8/31/72</u>
<u>A. Phillips</u>	<u>8/31/72</u>
_____	_____

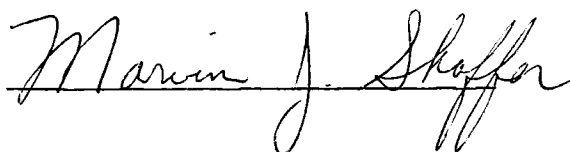
*This approval and acceptance is contingent on the candidate's adequate performance and defense of this dissertation at the final oral examination. The inclusion of this sheet bound into the library copy of the dissertation is evidence of satisfactory performance at the final examination.

STATEMENT BY AUTHOR

This dissertation has been submitted in partial fulfillment of requirements for an advanced degree at The University of Arizona and is deposited in the University Library to be made available to borrowers under rules of the Library.

Brief quotations from this dissertation are allowable without special permission, provided that accurate acknowledgment of source is made. Requests for permission for extended quotation from or reproduction of this manuscript in whole or in part may be granted by the head of the major department or the Dean of the Graduate College when in his judgment the proposed use of the material is in the interests of scholarship. In all other instances, however, permission must be obtained from the author.

SIGNED:

A handwritten signature in cursive script, reading "Marvin J. Shaffer", written over a horizontal line.

ACKNOWLEDGMENTS

Much appreciation and thanks are extended to Dr. Gordon R. Dutt for his assistance and direction in the pursuit of this program.

Thanks are expressed to the members of my committee, Dr. Daniel D. Evans, Dr. Robert A. Phillips, Dr. Wallace H. Fuller, and Dr. Hinrich L. Bohn for their time and help.

I wish to extend my thanks to the personnel of The University Computer Center for the use of their Multiple Linear Regression Program.

The author is indebted to the United States Department of the Interior, Bureau of Reclamation, and the IBP Desert Biome for funds provided in support of this research under contracts 5010-4151-11 and 5010-4151-17, and 5020-4151-16, respectively.

Finally, I would like to thank Miss Elvia Niebla for her assistance in many of the routine laboratory analyses.

TABLE OF CONTENTS

	Page
LIST OF TABLES	vi
LIST OF ILLUSTRATIONS	viii
ABSTRACT	ix
INTRODUCTION	1
LITERATURE REVIEW	4
Intermediates	6
Oxygen	7
Moisture and Salt Content	7
pH	8
Ammonium	9
Nitrification Models	10
Miyake Model	10
Quastel and Scholefield Model	11
Downing, Painter, and Knowles Model	12
Sabey, Frederick, and Bartholomew Model	14
McLaren Model	15
Shaffer, Dutt, and Moore Model	17
THEORY	20
Transition State	20
Derivation of Rate Expression	
Containing Partition Functions	21
Partition Functions for Ideal Gases	26
Reactions in Solution	28
Dielectric Constant of Solvent	29
Ionic Strength	29
Soil pH	30
Hydrostatic Pressure	31
EXPERIMENTAL MATERIALS AND METHODS	33
Soils	33
Nitrogen Source	34
Soil Analyses	34
Incubation Study	36
Ammonium Exchange Study	38
pH Study	39

TABLE OF CONTENTS--Continued

	Page
RESULTS AND DISCUSSION	41
Ammonium and Oxygen	41
pH	45
Partition Functions	50
Partition Function for O_2	50
Partition Function for H^+	52
Partition Function for NH_4^+	53
Partition Function for NH_2OH	55
Partition Function for N_2O	56
Partition Function for NO_2^-	58
Comparison of Equation Forms and Activated Complexes	60
The Rate Model	68
Basic Assumptions	69
Computer Program	70
Application of Nitrification Rate Model to Panoche and Desert Soils	71
Additional Verification of Nitrification Rate Model	76
SUMMARY AND CONCLUSIONS	89
APPENDIX A: COMPUTER LISTING OF RATE SUBROUTINE . . .	92
APPENDIX B: COMPUTER LISTING OF GENERAL COMPUTATIONAL PROGRAM	97
APPENDIX C: DATA COLLECTED IN INCUBATION STUDY . . .	103
LITERATURE CITED	108

LIST OF TABLES

Table	Page
1. Some Chemical and Physical Properties of the Panoche and Desert Soils	35
2. Some Chemical and Physical Properties of the Parshall and Gardena Soils	37
3. Correlations for Nitrification Reaction Rates versus $N_{NH_4}^+$ Concentrations	42
4. Correlations for Nitrification Reaction Rates versus $N_{NH_4}^+$ Activities	42
5. Calculated and Observed Values for Percent of $N_{NH_4}^+$ on the Exchange Complex	44
6. Calculated and Observed pH Values for Panoche and Desert Soils	48
7. Calculated and Observed pH Values for Panoche and Desert Soils Treated with HCl	51
8. Data for Rotational and Vibrational Partition Functions for O_2	52
9. Wave Lengths of Vibrational Modes for NH_4^+	54
10. Wave Lengths of Vibrational Modes for NH_2OH	57
11. Data for Rotational and Vibrational Partition Functions for NO_2	59
12. Partition Functions and Statistical Data for Equation (73) and Panoche Soil	64
13. Partition Functions and Statistical Data for Equation (74) and Panoche Soil	65
14. Partition Functions and Statistical Data for Equation (73) and Desert Soil	66
15. Partition Functions and Statistical Data for Equation (74) and Desert Soil	67

LIST OF TABLES--Continued

Table	Page
16. Statistical Data from Pairing Calculated and Observed Rates for the Panoche and Desert Soils	75
17. Calculated and Observed Nitrification Rates for the Parshall and Gardena Soils	77
18. Statistical Data from Pairing Calculated and Observed Nitrification Rates for the Parshall and Gardena Soils	78
19. Estimated Soil Extract Analyses Used in Verification of Nitrification Model	86
20. Statistical Data for $N_{NH_4^+}$ Saturation Values in Parshall Soil	87
21. Statistical Data for $N_{NH_4^+}$ Saturation Values in Gardena Soil	88

LIST OF ILLUSTRATIONS

Figure	Page
1. Potential Energy Versus Reaction Coordinate for a Typical Exothermic Chemical Reaction	22
2. Percent of $N_{NH_4}^+$ on the Exchange Complex as a Function of Moisture Content	40
3. Block Diagram of Computerized Rate Subroutine	72
4. Relationship of Activation Energy to Ionic Strength for Panoche and Desert Soils	73
5. Calculated and Observed Rate Data for Parshall Soil at Various Moistures after 10 Days Incubation	80
6. Calculated and Observed Rate Data for Parshall Soil at Various Moistures after 20 Days Incubation	81
7. Calculated and Observed Rate Data for Parshall Soil at Various Moistures after 40 Days Incubation	82
8. Calculated and Observed Rate Data for Gardena Soil at Various Moistures after 10 Days Incubation	83
9. Calculated and Observed Rate Data for Gardena Soil at Various Moistures after 20 Days Incubation	84

ABSTRACT

Transition state theory was applied to the nitrification process in soil-water systems, and a computerized, theoretical rate model was developed to include NH_4^+ and O_2 concentrations, pH, temperature, moisture content, and local differences in nitrifying capacities of Nitrosomonas bacteria.

The model was restricted to enriched calcareous soils thus simplifying the application of basic physicochemical principles. Experimental rate data from an agricultural and a native desert soil provided verification of a zero order reaction for nitrification with respect to NH_4^+ concentrations above a certain saturation level, as previously reported. The saturation concentration in soils was found to be about 1.0 to 5.0 ppm.

A theoretical linear relationship between activation energy and ionic strength was confirmed by application of the above data. However, each local population of nitrifiers tended to display different values for the slope and intercept of the linear relationship.

The structure of the activated complex for NH_4^+ oxidation to NO_2^- was determined to be more like NH_2OH or NH_4^+ than NO_2^- . As a first approximation, the NH_2OH

activated complex was included in the rate model. The equation form for the equilibrium between the reactants and the activated complex was found to differ from the stoichiometric reaction between NH_4^+ and O_2 to form NH_2OH . The equilibrium expression was found to be more closely approximated by the relationship, $2 \text{NH}_4^+ + \text{O}_2 \rightleftharpoons (\text{ACTIVATED COMPLEX})^+ + \text{H}^+$.

A method was developed to compute soil pH values as a function of moisture content. Verification was obtained by using data obtained from the agricultural and native desert soils, including cases where samples were acidified. The calculated pH values were used in the nitrification rate model.

Further verification of the model was obtained using data from the literature for two soils from the Northern Great Plains. Data pairing of observed and predicted rates for these soils yielded R values of 0.944 and 0.940.

The rate model was programmed in FORTRAN IV computer language and designed to operate in conjunction with existing computer models. Thus, this relatively sophisticated model may be applied to field simulation studies with a minimum of adaptive procedures. The model should aid in obtaining reliable predictions of NO_3^- formation and movement under a wide range of field conditions.

INTRODUCTION

Nitrogen pollution of streams, lakes, and groundwater has become a topic of considerable discussion in hydrology and related disciplines in recent years. N pollution sources may include municipal sewage effluents and various aspects of agriculture including cattle feed lots and overuse of commercial fertilizers in crop production. Also, native geologic deposits of NO_3^- are a source of N contamination.

Unborn children and infants are quite susceptible to methemoglobinemia, a disease related to NO_3^- in water and food supplies. NO_2^- is actually responsible for the disease, but NO_3^- can be reduced to NO_2^- by coliform microorganisms in the digestive tract. Methemoglobin is formed by the reaction of NO_2^- with oxyhemoglobin in the blood. Unlike oxyhemoglobin, methemoglobin cannot transport oxygen resulting in "blue babies." Similarly, livestock, particularly ruminants, which consume water or feed containing appreciable quantities of NO_3^- , are susceptible to methemoglobinemia.

Algal blooms may occur in lakes and streams when sufficient NO_3^- and other nutrients are present. These organisms may then die and the resulting decay processes may

remove the dissolved oxygen from the water and kill or exclude the fish population.

Crop production may be adversely affected by NO_3^- and NH_4^+ concentrations in the root zone which are too high or too low depending on the stage of growth. Also, NO_2^- toxicity to plant growth has been noted even at low NO_2^- concentrations.

The process of converting NH_4^+ to NO_2^- and NO_3^- is known as nitrification. This is a microbial process accomplished almost exclusively by bacteria of the genera Nitrosomonas ($\text{NH}_4^+ \rightarrow \text{NO}_2^-$) and Nitrobacter ($\text{NO}_2^- \rightarrow \text{NO}_3^-$). Since nitrification is such an important process with respect to N pollution and in other areas such as soil fertility and plant nutrition, the continued development of descriptive mathematical models seems highly desirable. These aid environmental impact studies, help to improve fertilizer efficiencies, and provide a better basic understanding of the nitrification process.

Several attempts have already been made to model nitrification. However, since nitrogen chemistry is very complex, the models to date, in part, have been overly simplified and/or empirical. The need exists for a more detailed model capable of adequately describing the process as it occurs under field conditions.

This paper reports on the development of a transition state, rate process theory, model of nitrification in

soil-water systems. This represents the first known attempt to apply transition state concepts to the nitrification process. The model is designed to approximate the nitrification rate process under a range of temperatures, moisture contents, NH_4^+ , O_2 , and H^+ concentrations, and salt levels common in soils under field situations. The model can be used in conjunction with existing models (e.g., Dutt, Shaffer, and Moore, 1972) to predict the NH_4^+ , NO_3^- , urea, and organic N concentrations in soil-water systems and associated leachates.

LITERATURE REVIEW

Schloessing and Muntz (1877) were the first to show that nitrification in soil-water systems is a microbial process. Their experiment consisted of application of sewage effluent to a column of sand and chalk. Analyses of the applied sewage and leachate from the column indicated conversion of the input NH_4^+ to NO_3^- . The process was inhibited by chloroform, but restored by washings with sterile water followed by applications of washings from soil. The conclusion was made that the process was microbial.

In the early 1890's, Frankland and Frankland (1890), Warington (1891), and Winogradsky (1890) independently isolated the NH_4^+ oxidizing microorganisms. In addition, Winogradsky (1890) isolated the NO_2^- microorganisms. These results established the two stage nature of the nitrification process.

Stevens and Withers (1909) compared the nitrification rate of NH_4^+ in soil with that obtained in solution culture. A more rapid rate was observed in soil suggesting possible influences of solid phase materials. Miyake (1916) and Pulley and Greaves (1932) found that NO_3^- concentration as a function of time follows a sigmoid type curve for the nitrification process. Caster, Martin, and Buehrer (1942),

Fraps and Sturges (1939), and Pikovskaya (1940) showed that nitrifying microorganisms isolated from different soils have different nitrifying capacities.

Intermediate products in the nitrification process were studied at early dates. The presence of hyponitrous acid in solution culture during nitrification was demonstrated by Beesley (1914) and Corbet (1935). Hydroxylamine was suggested as a possible intermediate by Kluyver and Donker (1925).

Lees and Quastel (1946) introduced the method and apparatus for soil perfusion studies. Soil perfusion techniques treat the soil as a biological whole, much as if it were a living plant or animal tissue. Changes within the soil during the experiment are observed under a specified set of conditions. Lees and Quastel (1946) first applied the soil perfusion techniques to the study of nitrification. These same authors determined that nitrifying bacteria grow on the surfaces of clay particles and utilize adsorbed NH_4^+ .

Quastel and Scholefield (1951) noted that nitrifying bacteria eventually reach a state in which all the available sites for growth are saturated with nitrifying microorganisms. In this saturated state, the soil is said to be "enriched." Also, the same authors noted that an enriched soil shows no initial lag period during the nitrification process.

Intermediates

Various intermediate compounds have been suggested in the nitrification pathway between NH_4^+ and NO_2^- . The most frequently studied are hydroxylamine, hyponitrite, and nitrohydroxylamine. Yoshida and Alexander (1964) demonstrated that hydroxylamine is formed by Nitrosomonas europaea. Nicholus and Jones (1960) found that the cells of Nitrosomonas contain the enzyme for conversion of hydroxylamine probably serves as a precursor to NO_2^- . The same authors found that when high concentrations of hydroxylamine are being oxidized to NO_2^- , N_2O and some NO and NO_2 are evolved. However, the N_2O was not oxidized to NO_2^- , and the conclusion was made that N_2O is an unlikely intermediate in the nitrification process.

Hofman and Lees (1953), and Yoshida and Alexander (1964) found that hydrazine is an inhibitor of the conversion of hydroxylamine to NO_2^- . Alexander (1961) suggested that hyponitrite might be an intermediate between hydroxylamine and NO_2^- . Campbell and Lees (1967) pointed out that hyponitrite is not oxidized by Nitrosomonas and therefore is not a likely intermediate. These same authors suggested nitrohydroxylamine ($\text{NO}_2\cdot\text{NH}\cdot\text{OH}$) as a likely intermediate. Also, they mentioned nitroxyl (NOH) and nitramide ($\text{NO}_2\cdot\text{NH}_2$) as possible but unlikely intermediates.

Oxygen

Aerobic conditions are required for the oxidation of NH_4^+ to NO_2^- and NO_3^- . Longmuir (1954), Griffin (1963), Greenwood (1968), and Macauley and Griffin (1969) all noted that aerobic respiration is unimpeded by lowering oxygen partial pressures until exceptionally low values occur at the microbial surfaces.

Greenwood (1962) found that nitrification in solution is not inhibited by oxygen concentrations until they drop to below 0.16 mg/L. Boon and Laudelout (1962) found the Michaelis saturation constant K_m for oxygen is about 0.25 mg/L at 18° C and 0.5 mg/L at 32°C. The apparent upper limit for the effect of oxygen concentrations on the nitrification process can be explained by the enzymatic nature of the process as noted by McLaren (1970).

Moisture and Salt Content

The effect of moisture and salt on nitrification has received considerable attention. Parker and Larson (1962) found inhibition of nitrification at soil moisture contents less than 0.05 bar suction. Justice and Smith (1962) observed no nitrification at moisture contents below 115 bars suction, with increased rates at higher moisture contents. Miller and Johnson (1964) observed a peak in nitrification rates at 0.50 to 0.15 bar suction. Robinson (1957) found that nitrification did not occur at moisture contents less than one-half the permanent wilting percentage. Shaffer

(1970) found that nitrification rates in soils are independent of moisture content at moistures greater than about 10 bars suction.

Although it is difficult or impossible to separate moisture effects from purely osmotic effects, several authors have determined nitrification rates as a function of osmotic pressure. Johnson and Guenzi (1963) found that increased osmotic tension reduced nitrification rates in a linear manner in soil-water systems. Also, these same authors found that nitrifiers in different soils show different tolerances to salt content. Reichman, Grunes, and Viets (1966) showed that nitrification rates in soils decrease as the moisture contents decrease and the osmotic tensions increase.

pH

The effects of pH on nitrification are well known. Since H^+ is formed during the oxidation of NH_4^+ , the pH tends to fall as nitrification progresses. This in turn may inhibit the reaction unless pH buffering takes place.

Meyerhof (1916) found that the optimum pH for Nitrosomonas is 8.5 to 8.8, while for Nitrobacter, 8.3 to 9.3. Quastel and Scholefield (1951) noted that the optimum pH for nitrification in pure culture is 8.5, while the lower limit was placed at 4.0. These same author found that a soil with pH 4.5 did not oxidize NH_4^+ .

Broadbent, Tyler, and Hill (1957) found that NH_4^+ is oxidized more rapidly in soils which are amended with OH^- .

These authors also noted inhibition of Nitrobacter at 800 ppm $N_{NH_4^+}$ in alkaline soils. This may have been due to the deleterious effects of free ammonia on these microorganisms. The accumulation of NO_2^- following field application of NH_4^+ to alkaline calcareous soils has been reported by Fuller, Martin, and McGeorge (1950).

Caster et al. (1942) found a threshold pH of 7.6 to 7.8 above which there is no NO_2^- oxidation to NO_3^- . Broadbent et al. (1957) found that oxidation of NH_4^+ becomes very slow near pH 5.0.

Ammonium

The effect of NH_4^+ concentrations on nitrification rates has been the subject of many articles. Stojanovic and Alexander (1958) pointed out that high NH_4^+ concentrations have little effect on the rate of NH_4^+ oxidation to NO_2^- , but that high NH_4^+ tends to suppress the conversion of NO_2^- to NO_3^- . Broadbent et al. (1957) found that under low NH_4^+ concentrations and other conducive conditions, conversion of NH_4^+ to NO_3^- proceeds rapidly to completion. McIntosh and Frederick (1958) concluded that NO_3^- formation from NH_4^+ takes place more rapidly where the NH_4^+ concentration is less than 400 ppm.

McLaren (1970) noted that nitrification rates in enriched soils are first order with respect to substrate at low substrate concentrations. In the case of NH_4^+ oxidation

to NO_2^- , Knowles, Downing, and Barrett (1965) placed the boundary between high and low NH_4^+ concentrations at about 1 ppm $\text{N}_{\text{NH}_4^+}$. Boon and Laudelout (1962), and Laudelout and Tichelen (1960) gave values of 23 and 9 ppm $\text{N}_{\text{NO}_2^-}$, respectively for a similar boundary in the case of NO_2^- oxidation to NO_3^- .

The zero order nature of the nitrification process in enriched soils with high $\text{N}_{\text{NH}_4^+}$ concentrations has been given a theoretical basis by McLaren (1970). Also, the same author noted that growing populations of nitrifiers may exhibit maximum growth rates at high substrate concentrations. It is not known whether the boundaries between high and low substrate concentrations previously mentioned apply equally to enriched and unenriched soils.

Nitrification Models

Several mathematical relationships have been proposed to describe nitrification in soil-water systems. All of these to date have either been simplified models for nitrification under specific, limited conditions or semi-empirical models for nitrification under a wider range of conditions. A review is presented here to demonstrate some attributes and deficiencies inherent in these models.

Miyake Model

Miyake (1916) proposed the following equation describing nitrification in soils

$$Y = (A'' - Y) \exp(K(t - t_1)) \quad (1)$$

where Y is the $N_{NO_3^-}$ produced

A'' is the asymptotic value approached by Y

t is time

t_1 is time to $Y = A''/2$

K is a constant.

This equation fits the classic sigmoid curve observed when soils with less than maximal populations of nitrifying microorganisms are incubated under conditions conducive to microbial activity. The equation does not apply to initially enriched soils, which lack the lag portion of the sigmoid curve. In addition, the equation does not allow for changes in pH, NH_4^+ and O_2 concentrations, temperature, and moisture content.

Quastel and Scholefield Model

Quastel and Scholefield (1951) derived the following relationship for nitrification in soils

$$Y = \underline{K}' \exp(Ct) \quad (2)$$

where Y is the $N_{NO_3^-}$ produced

t is time

\underline{K}' and C are constants.

The equation has the boundary condition that $Y=0$ when $t=0$. It models the lag and the essentially constant rate portion of the experimentally observed sigmoid nitrification curve. The model does not account for limiting NH_4^+ concentrations

nor does it allow changes in pH, O_2 concentration, temperature, and moisture and salt content.

Downing, Painter, and Knowles Model

Downing, Painter, and Knowles (1964) published an integrated form of the Michaelis (e.g., McLaren, 1970) type equation for nitrification in river water. These authors related mass of $N_{NH_4^+}$ produced to dry mass of Nitrosomonas organisms by using the expression

$$C_m - C_m^0 = E_m (N_{NH_4^+}^0 - N_{NH_4^+}) \quad (3)$$

where C_m is the concentration of Nitrosomonas

$N_{NH_4^+}^0$ is the initial $N_{NH_4^+}$ concentration

$N_{NH_4^+}$ is the $N_{NH_4^+}$ concentration

C_m^0 is the initial concentration of
Nitrosomonas

E_m is the dry mass of Nitrosomonas produced
per oxidation of unit mass of $N_{NH_4^+}$

Combination of this equation with the Michaelis equation in the form

$$\frac{d N_{NH_4^+}}{dt} = \frac{\underline{K}'' C_m N_{NH_4^+}}{K_m + N_{NH_4^+}} \quad (4)$$

where \underline{K}'' is the growth rate constant

K_m is the Michaelis constant

t is time.

yields the following expression upon integration

$$\underline{K}''t - 1/A' = E_m K_m \ln (N_{\text{NH}_4^{\circ}}/N_{\text{NH}_4^+}) + (A' - E_m K_m) \ln [(A' - E_m K_m)/C_m^{\circ}] \quad (5)$$

$$\text{where } A' = C_m^{\circ} + E_m N_{\text{NH}_4^{\circ}} \quad (6)$$

Knowles et al. (1965) determined values for \underline{K}'' , C_m , and K_m . They used a trial procedure and a digital computer program together with experimental values for $N_{\text{NH}_4^+}$ and $N_{\text{NH}_4^{\circ}}$. The value for E_m was taken as 0.05. To account for changes in \underline{K}'' as a function of temperature, a regression equation was derived and may be written

$$\log \underline{K}'' = 0.0413T - 0.944 \quad (7)$$

where T is temperature

\underline{K}'' has units of days⁻¹.

Also, an expression relating the Michaelis constant K_m to temperature was derived in a similar manner and may be written

$$\log K_m = 0.051T - 1.158 \quad (8)$$

where K_m has units of mg/L $N_{\text{NH}_4^+}$.

No equations were presented for the variation in \underline{K}'' and K_m with changes in O_2 and H^+ concentrations. The authors noted that \underline{K}'' is independent of O_2 concentration above about 2 mg/L O_2 .

This model incorporates empirical regression equations to account for the effects of temperature variation on a Michaelis type rate equation. The data used to derive the regression equations were taken from samples of river water

containing soil particles. Different expressions might be expected for lower moisture contents encountered in soils under field conditions. In addition, pH, limiting NH_4^+ and O_2 concentrations, and salt effects were not considered.

Sabey, Frederick, and Bartholomew Model

The amount of nitrate nitrogen accumulating in time may be described by the following equation proposed by Sabey, Frederick, and Bartholomew (1969)

$$N_{\text{NO}_3^-} = K_f R_k (t - t_f r_t) \quad (9)$$

where t is time

K_f is the characteristic nitrifying capacity

R_k is a composite factor or rate index based on the relative maximum $N_{\text{NO}_3^-}$ accumulation rates under less favorable conditions of moisture, temperature, pH, texture, aeration, etc.

t_f is the characteristic delay period under optimum conditions

r_t is a composite factor or delay index based on the relative delay periods under less favorable conditions

$$\text{where } R_k = R_t R_{\bar{m}} R_{\text{pH}} R_{\text{tex}} R_a R_x \quad (10)$$

$$r_t = r_t r_{\bar{m}} r_{\text{pH}} r_{\text{tex}} r_a r_p r_x \quad (11)$$

where R_t , etc. are relative rate indexes, r_t , etc. are relative delay indexes, and

where the subscript

t is temperature

\bar{m} is moisture

pH is pH

tex is texture

a is aeration

p is population of nitrifiers

x is a composite of all other influential factors.

This model incorporates many of the variables known to influence nitrification rates in soil-water systems. However, the manner in which the variables are interrelated appears to be rather empirical. The model could yield useful predictions provided values for the respective indexes can be determined. The authors did not present values for more than three of the indexes.

McLaren Model

McLaren (1970) proposed the following equation for NH_4^+ oxidation rates in soils (similar expressions were given for NO_2^- oxidation, etc.)

$$-\frac{d(\text{NH}_4^+)}{dt} = \frac{\bar{A}d\hat{M}}{dt} + \gamma\hat{M} + \frac{K'''\beta\hat{M}(\text{NH}_4^+)}{K_m + (\text{NH}_4^+)} \quad (12)$$

where NH_4^+ is the substrate (NH_4^+) concentration
 \hat{M} is biomass
 \bar{A} , γ , and \bar{B} are proportionality constants
 K_m is the saturation (Michaelis) constant
 K''' is the specific rate constant.

The first term in equation (12) is the Monod growth rate expression for microorganisms, the second is the Pirt maintenance term, and the third represents oxidation of the NH_4^+ due to the enzyme system. At small NH_4^+ concentrations and in a fully enriched soil (e.g., a soil in which the Nitrosomonas population is maximal and constant), equation (12) can be written

$$-\frac{d(\text{NH}_4^+)}{dt} = \gamma \hat{M}_{\max} + \underline{K}(\text{NH}_4^+) \quad (13)$$

$$\text{where } \underline{K} = K' \hat{B} \hat{M}_{\max} / K_m \quad (14)$$

For large NH_4^+ concentrations equation (12) becomes

$$-\frac{d(\text{NH}_4^+)}{dt} = \gamma \hat{M}_{\max} + K' \hat{B} \hat{M}_{\max} = v \quad (15)$$

where v is a constant.

McLaren (1971) developed an equation for NH_4^+ oxidation rates in soils with populations $\ll \hat{M}_{\max}$ and large NH_4^+ concentrations. Here

$$\gamma = \frac{\gamma_{\infty}(\text{NH}_4^+)}{K_g + (\text{NH}_4^+)} \quad (16)$$

where γ_{∞} and K_g are characteristic growth constants for Nitrosomonas,

$$\text{which reduces to } \gamma = \gamma_{\infty} \quad (17)$$

at large NH_4^+ concentrations. Also

$$\hat{M} = \hat{M}_0 \exp(\gamma_{\infty} t) \quad (18)$$

where \hat{M}_0 is the initial biomass
 t is time.

$$\text{If } \frac{d\hat{M}}{dt} = \gamma\hat{M}(1 - \hat{M}/\hat{M}_{\max}) \quad (19)$$

(Lees and Quastel, 1946), then at large NH_4^+ concentrations
 and $\hat{M} \ll \hat{M}_{\max}$

$$\frac{-d(\text{NH}_4^+)}{dt} = \underline{C}M_0 \exp(\gamma_{\infty}t) \quad (20)$$

where \underline{C} is a constant.

McLaren's model incorporates microbial growth and maintenance relationships as well as the Michaelis relationship describing enzyme catalyzed processes such as nitrification. His model should apply to soil-water systems with submaximal as well as maximal populations of nitrifiers. However, McLaren did not include temperature as a variable (a drawback in the Michaelis approach) nor did he consider the effects of pH/oxygen concentration or moisture content. These variables would have to be held constant whenever the constants in McLaren's model are determined. Since the variables mentioned tend to vary in soil-water systems under field conditions, McLaren's model is not yet applicable to the field.

Shaffer, Dutt, and Moore Model

Shaffer, Dutt, and Moore (1969) used a semi-empirical approach involving a multiple linear regression analysis

of published data for several alkaline soils to derive the following equation for nitrification rates in soil-water systems

$$\frac{d\text{NH}_4^+}{dt} = 4.64 + 1.62 \cdot 10^{-3} T (\text{N}_{\text{NH}_4^+}) + \quad (21)$$

$$4.50 \log (\text{N}_{\text{NH}_4^+}) - 2.51 \log (\text{N}_{\text{NO}_3^-})$$

where T is temperature

$\text{N}_{\text{NH}_4^+}$ is the $\text{N}_{\text{NH}_4^+}$ concentration

$\text{N}_{\text{NO}_3^-}$ is the $\text{N}_{\text{NO}_3^-}$ concentration.

Adjustments were made to rates computed by this equation to account for effects due to moisture contents below 10 bars suction. The following assumptions were made to allow application of this model to the field situation.

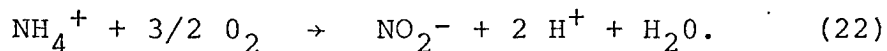
1. The soil moisture content remains in the range approximately bounded by field capacity and permanent wilting point.
2. The soil pH remains in the range 7.0 to 8.5.
3. Denitrification is insignificant.
4. Gaseous losses of NH_3 are insignificant.
5. Fixation of N_2 gas is insignificant.
6. Nitrification rate is unaffected by ionic strength.
7. Different microbial populations respond about equally to the input variables.

8. The response of microorganisms to pH is about the same from pH 7.0 to 8.51
9. Fixation of NH_4^+ in clay lattices is insignificant.
10. The effects of varying O_2 partial pressures are insignificant.
11. NO_2^- accumulation is insignificant.

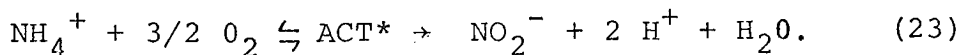
THEORY

Transition State

Consider the reaction for NH_4^+ oxidation to NO_2^-



A plot of the potential energy curve for a typical exothermic reaction such as NH_4^+ oxidation, equation (22), appears in Figure 1. The energy of activation, ΔE_c , (or ΔE_0 if zero point energies are included) represents the highest energy barrier which must be overcome between the reactants (e.g., NH_4^+ and O_2) and products (e.g., NO_2^- , H^+ , and H_2O). If the assumption is made that a transition state or activated complex at the top of the energy barrier is in equilibrium with the reactants, then equation (22) becomes



Another basic assumption of transition state theory states that the rate of reaction is first order with respect to the activated complex. Thus for equation (23) (Stevens, 1970)

$$-\frac{d\text{NH}_4^+}{dt} = \nu \text{ACT}^* \quad (24)$$

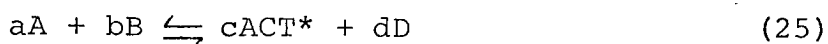
where ν is the frequency per unit time with which the activated complexes cross the barrier to form products

ACT^* is the concentration of the activated complex (number/unit volume).

ΔG in Figure 1 represents the free energy change associated with the overall reaction. For NH_4^+ oxidation to NO_2^- , ΔG is about -66.5 Kcal/mole.

Derivation of Rate Expression Containing Partition Functions

The values of ν and ACT^* can be obtained as follows. For clarity consider a general reaction of the form



Then from statistical thermodynamics (Hill, 1960)

$$\frac{\rho_{\text{ACT}^*}^c \rho_D^d}{\rho_A^a \rho_B^b} = \frac{\left[\frac{q_{\text{ACT}^*}}{V} \right]^c \left[\frac{q_D}{V} \right]^d}{\left[\frac{q_A}{V} \right]^a \left[\frac{q_B}{V} \right]^b} = K_{\text{eq}} \quad (26)$$

where ρ is the number density (number of molecules or ions/unit volume) for the specie indicated by the subscript

q is the partition function for the specie indicated by the subscript

V is volume

K_{eq} is the equilibrium constant for the reaction represented by equation (25).

In general, the q 's appearing in equation (26) are products of their component partition functions. Thus,

$$q(\text{total}) = q_{\text{tran}} q_{\text{rot}} q_{\text{vib}} q_{\text{ele}} \quad (27)$$

where $q(\text{total})$ is the total partition function for the particular specie

q_{tran} is the partition function for translational motion

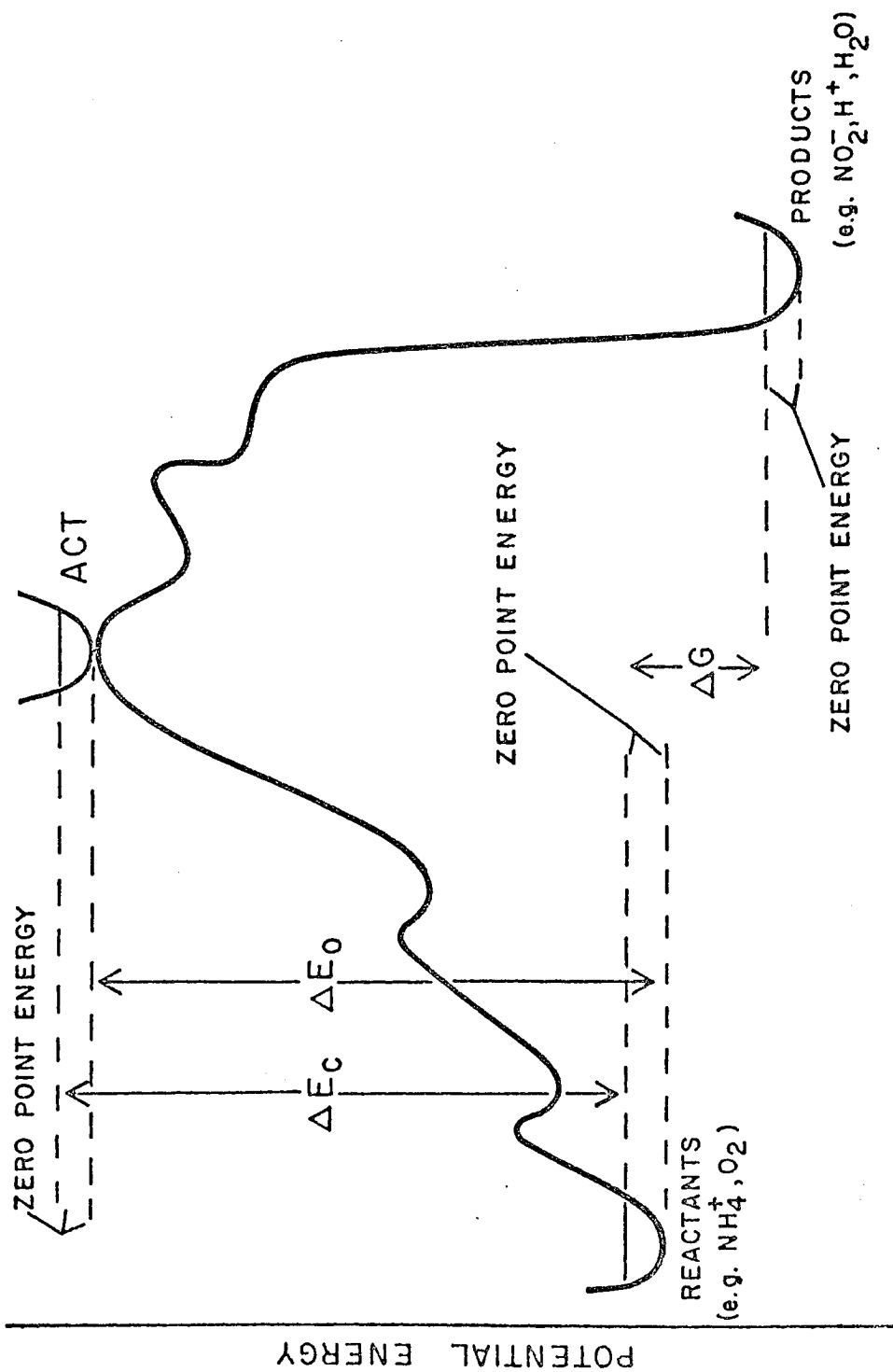


Figure 1. Potential Energy Versus Reaction Coordinate for a Typical Exothermic Chemical Reaction.

q_{rot} , rotational motion
 q_{vib} , vibrational motion
 q_{ele} , electronic motion.

Other partition functions may be included here (such as q_{atomic}) but usually make insignificant contributions to the total function at ordinary temperatures.

Motion along the reaction coordinate (or pathway between the reactants and products in potential energy space) at the activated complex is treated as translational motion in one dimension. The assumption is made that one normal mode of vibrational freedom is directed along the reaction coordinate. This vibrational mode is usually the mode associated with the weakest bond. Thus

$$q_{\text{ACT}^*} = q_{\text{tran}} q_{\text{rot}} q_{\text{vib}^*} q_z q_{\text{ele}} \quad (28)$$

where q_{ACT^*} is the partition function for the activated complex

q_z is the partition function for the reaction coordinate

q_{vib^*} is the vibrational partition function less one mode of vibrational freedom.

The expression of q_z may be written

$$q_z = \Delta z \sqrt{\frac{2\pi M^* kT}{h^2}} \quad (29)$$

where Δz is the length along the reaction coordinate

M^* is the mass of the activated complex

k is Boltzmann's constant

T is temperature

h is Planck's constant.

This expression is the classical representation for translational motion in one dimension.

Let \dot{v} be the velocity along the reaction coordinate. If $\dot{v} < 0$, the reaction is assumed to proceed. If $\dot{v} > 0$, the reaction does not take place. The fraction of all activated complexes with \dot{v} 's in the range \dot{v} to $\dot{v} + d\dot{v}$ may be expressed (Hill, 1960)

$$p(\dot{v})d\dot{v} = \frac{\exp\left(-\frac{\beta}{2} M^* \dot{v}^2\right) d\dot{v}}{\int_{-\infty}^{\infty} \exp\left(-\frac{\beta}{2} M^* \dot{v}^2\right) d\dot{v}} \quad (30)$$

where $P(\dot{v})d\dot{v}$ is the probability of finding an activated complex with velocity \dot{v} to $d\dot{v}$

β is $1/kT$.

The denominator of equation (30) may be integrated in closed form to give

$$p(\dot{v})d\dot{v} = \sqrt{\frac{M^*}{2\pi kT}} \exp\left(-\frac{\beta}{2} M^* \dot{v}^2\right) d\dot{v} \quad (31)$$

An activated complex with velocity \dot{v} must be within a distance \dot{v} to cross the barrier in unit time. Let ρ' be the number of activated complexes per unit length and per unit volume along the reaction coordinate. Then, $\rho' \dot{v}$ is the number of activated complexes crossing the barrier per unit time with velocity \dot{v} . The expression for the total number

of activated complexes crossing the barrier per unit time at any velocity > 0 is (Hill, 1960)

$$\text{Rate} = \int_0^{\infty} \rho' \dot{v} p(\dot{v}) d\dot{v} \quad (32)$$

where Rate is the rate of reaction.

Combining this equation with equation (31) and integrating gives

$$\text{Rate} = \rho' \sqrt{\frac{M^*}{2\pi kT}} \cdot \frac{kT}{M^*} = \rho' \sqrt{\frac{kT}{2\pi M^*}} \quad (33)$$

Also, $\Delta z \rho'$ is the number of activated complexes per unit volume of the system (not per unit volume along the reaction coordinate at the activated state.) Combining this result with equations (26) and (33) yields

$$\frac{(\Delta z \rho')^c \rho_D^d}{\rho_A^a \rho_B^b} = \frac{\left[(q_{ACT}^1 \sqrt{\frac{2\pi M^* kT}{h^2}} \Delta z) / V \right]^c \left(\frac{q_D}{V} \right)^d}{\left(\frac{q_A}{V} \right)^a \left(\frac{q_B}{V} \right)^b} \quad (34)$$

where q_{ACT}^1 is the total partition function for the activated complex with q_z removed.

By removing the electronic portions of each partition function in equation (34) and combining them into a single expression, the exponential is now included in the rate expression which may be written

$$\text{Rate} = \frac{kT}{h} \cdot \frac{\frac{q_{\text{ACT}}''}{V} \left(\frac{q_D'}{V}\right)^{d/c}}{\left(\frac{q_A^1}{V}\right)^{a/c} \left(\frac{q_B^1}{V}\right)^{b/c}} \cdot \frac{\rho_A^{a/c} \rho_B^{b/c}}{\rho_D^{d/c}} \quad (35)$$

$$\exp[-\Delta E_c / (kT)]$$

where ΔE_c is the energy of activation with the zero point energies excluded

' denotes the partition function less the electronic contribution

$\frac{kT}{h}$ is ν and the remaining right side of the equation is $\sim \text{ACT}^*$ (see equation, 24).

Partition Functions for Ideal Gases

Use of activity coefficients allows the application of existing partition functions for ideal gases to nonideal soil-water systems. The following is a detailed discussion of the translational, rotational, and vibrational parts of total partition functions for ideal gases. A total partition function may be defined as the probability of the occurrence of a specie in a particular volume. The parts of the total function may be thought of as contributions due to the particular motion being modeled, e.g., translational, vibrational, etc. The classical partition function for translation in 3-dimensional space is written (Amis, 1949)

$$q_{\text{tran}} = V \left(\frac{2\pi M kT}{h^2} \right)^{3/2} \quad (36)$$

where M is the mass of the specie being considered.

The rotational partition function for diatomic molecules is (Hill, 1960)

$$q_{\text{rot}} = T/(\sigma\theta_r) \quad (37)$$

where σ is the symmetry number

θ_r is the rotational temperature.

The symmetry number corresponds to the number of different ways a molecule or ion can achieve, by rotation, the same orientation in space. The rotational temperature has components associated with the moment of inertia about the center of mass. Monatomic gases do not display rotational degrees of freedom and therefore do not have rotational partition functions.

Polyatomic molecules possess a more complex rotational partition function as follows (Hill, 1960)

$$q_{\text{rot}} = \frac{\sqrt{\pi}}{\sigma} \left(\frac{T^3}{\theta_A \theta_B \theta_C} \right)^{1/2} \quad (38)$$

where θ_A , θ_B , θ_C are the rotational temperatures for the three principal moments of inertia.

The vibrational partition function for diatomic molecules is (Hill, 1960)

$$q_{\text{vib}} = \exp[-\theta_v/2T] / [1 - \exp(-\theta_v/T)] \quad (39)$$

where θ_v is the vibrational temperature.

The vibrational temperature is related to a vibrational frequency which can be calculated from quantum mechanics or deduced from vibrational spectra.

The vibrational partition function for polyatomic molecules

$$q_{\text{vib}} = \prod_i \exp[-\theta_{\text{v}_i}/(2T)] / [1 - \exp(-\theta_{\text{v}_i}/T)] \quad (40)$$

where θ_{v_i} is the vibrational temperature for the i th normal mode of vibration.

The vibrational temperatures can be determined from vibrational frequencies using

$$\theta_{\text{v}_i} = \nu_i h/k \quad (41)$$

where ν_i is the frequency of the i th mode.

The number of vibrational modes for nonlinear polyatomic molecules or ions is (Hill, 1960)

$$\text{Number of Modes} = 3n - 6 \quad (42)$$

where n is the number of nuclei.

For linear molecules or ions, the number of vibrational modes is

$$\text{Number of Modes} = 3n - 5 \quad (43)$$

Reactions in Solution

The general rate expression derived up to this point, equation (35), may be applied to chemical reactions in general. However, derivation of partition functions for the motions of molecules and ions in a nonideal condensed medium such as liquid water is a difficult task.

Another approach involves application of partition functions for motions of the reacting species in an ideal gas, together with activity coefficients for the solution phase.

Dielectric Constant of Solvent

The effect on the reaction rate due to changes in the dielectric constant can be calculated using existing relationships (e.g., Harris, 1966). However, changes in the dielectric constant in aqueous solutions usually contribute much less to rate changes than alterations in the total concentration of ionic species. For this reason, changes in the dielectric constant were ignored in the development of the rate model.

Ionic Strength

In aqueous solutions, one of the main environmental factors influencing the reaction rate is the ionic strength of the solution. Activity coefficients for charged species in solution may be approximated by the Debye-Hückel expression (Garrels and Christ, 1965)

$$-\log \gamma_i = \frac{z_i^2 (0.509) \mu^{1/2}}{1 + \mu^{1/2}} \quad (44)$$

where γ_i is the activity coefficient of the *i*th specie

z_i is the charge on the *i*th specie

μ is the ionic strength of the solution

Here

$$\mu = \frac{1}{2} \sum_i z_i^2 C_i \quad (45)$$

where C_i is the concentration of the i th specie.

Activity coefficients for neutral molecules in solution may be computed by the expression (Harris, 1966)

$$\log \gamma_i = \bar{K}_m u \quad (46)$$

where \bar{K}_m is a semi-empirical constant.

In practice activity coefficients will often cancel out of the rate expression leaving a somewhat simplified relationship for the variation of the rate constant and observed activation energy with ionic strength.

Soil pH

In calcareous soil-water systems, the following set of equations may be combined to form an expression for the hydrogen ion activity at equilibrium (Garrels and Christ, 1965)

$$\frac{[\text{H}_2\text{CO}_3]}{P_{\text{CO}_2}} = K_1 \quad (47)$$

$$\frac{[\text{H}^+][\text{HCO}_3^-]}{[\text{H}_2\text{CO}_3]} = K_2 \quad (48)$$

$$\frac{[\text{H}^+][\text{CO}_3^{=}]}{[\text{HCO}_3^-]} = K_3 \quad (49)$$

and

$$[\text{Ca}^{++}][\text{CO}_3^{=}] = K_{\text{sp}} \quad (50)$$

where P_{CO_2} is the partial pressure of CO_2

[] refers to the activity of the indicated specie

K_1 , K_2 , K_3 , and K_{sp} are constants.

These equations may be combined to yield

$$[H^+] = \sqrt{\frac{K_1 K_2 K_3 P_{CO_2} [Ca^{++}]}{K_{sp}}} \quad (51)$$

which reduces to $[H^+] = \sqrt{K_4 P_{CO_2} [Ca^{++}]}$ (52)

where K_4 is a combination of previous constants.

pH may then be determined by using the familiar equation

$$pH = -\log[H^+] \quad (53)$$

Hydrostatic Pressure

Variation of reaction rates in solution with changes in hydrostatic pressure can be calculated by using the approach developed by van't Hoff. The variation of an equilibrium constant such as K_{eq} with pressure may be expressed by the van't Hoff equation

$$\frac{\partial \ln K_{eq}}{\partial P} = - \frac{\Delta V^*}{RT} \quad (54)$$

where P is pressure

ΔV^* is the volume of activation

R is the gas constant

and (Laidler, 1963)

$$k_R = (kT/h) K_{eq} \quad (55)$$

where k_R is the rate constant.

If the assumption is made that ΔV^* is independent of pressure, equation (54) can be integrated after combination with equation (55) to yield

$$\ln k_R = \ln k_R^0 - \frac{\Delta V^* P}{RT} \quad (56)$$

where k_R^0 is the rate constant at zero pressure (close to the value at atmospheric pressure).

Since pressures on the order of several thousand lbs/in² are needed to produce significant changes in rate constants, the pressure effect can be neglected in applications to most soil-water systems.

Application of nitrification rate data for soils together with the theoretical rate expression, equation (35), and the activity coefficients just discussed should allow the development of a transition state model for nitrification in soil-water systems.

EXPERIMENTAL MATERIALS AND METHODS

Three studies were conducted on two soils to obtain data to develop the nitrification model. An incubation study provided nitrification rate data at various moisture contents, temperatures, NH_4^+ concentrations, and pH values. An NH_4^+ exchange study yielded data which were used to test an existing NH_4^+ exchange model. pH data from the third study allowed the development of a method to compute soil pH as a function of moisture content.

Nitrification rate data from the literature provided further verification of the completed rate model.

Soils

Five soils were included in this study. The first two, a Panoche fine sandy loam (Typic Torriorthent) from California and an unnamed gravelly loamy sand (Typic Torri-fluvent) from a desert area of Pima County, Arizona, were used in the incubation, NH_4^+ exchange, and pH studies. Data from the third and fourth soils, Parshall fine sandy loam and Gardena loam, both from the Northern Great Plains, were used to further verify the final, theoretical rate model. The fifth soil, an unnamed clay loam from the Page Ranch, Pima County, Arizona, was initially included in the incubation study. However, the soil did not develop a significant

population of nitrifiers until it had been incubated with an application of 400 $\mu\text{g/g N}_{\text{NH}_4^+}$, and at 25°C and 1/3 bar suction for about five months. As a result, time did not allow collection of rate data for this soil which could be used to develop or verify the nitrification model.

Nitrogen Source

Analytical reagent grade NH_4Cl (Mallinckrodt Chemical Works) was used as a source of nitrogen in the incubation, NH_4^+ exchange, and pH studies.

Soil Analyses

The Panoche and desert soils were analyzed by the author for the various parameters listed in Table 1. NH_4^+ and NO_3^- were determined using steam distillation techniques with MgO followed by Devarda's alloy. The Ca^{++} and Mg^{++} were run by application of the 1,2-diaminocyclohexane-N,N, N^1, N^1 -tetraacetic acid (DCyTA) method (Meites, 1963). Na^+ was determined using flame emission techniques. $\text{CO}_3^{=}$ and HCO_3^- concentrations were found by titration with H_2SO_4 to the phenolphthalein and methyl orange endpoints, respectively. Cl^- was determined using the Mohr method. $\text{SO}_4^{=}$ was run by application of the Thorin method (Brown, Skougstad, and Fishman, 1970).

Cation exchange capacity was determined using the $\text{NH}_4\text{OAc} - \text{NH}_4\text{NO}_3$ method described by Keeney and Bremner (1969). pH was determined with the soil particles in

Table 1. Some Chemical and Physical Properties of the Panoche and Desert Soils

Parameter	Units	Panoche	Desert
Composition of 1:5 Soil Water Extract			
	µg/g		
NH ₄ ⁺ -N		3.2	2.3
NO ₃ ⁻ -N		28.0	8.5
Ca ⁺⁺		277.	79.2
Mg ⁺⁺		50.8	32.8
Na ⁺		164.	17.3
HCO ₃ ⁻		147.	249.
CO ₃ ⁼		0.0	0.0
Cl ⁻		61.6	30.0
SO ₄ ⁼		1931.	84.3
Cation Exchange Capacity	meq/100 g	12.1	6.4
pH Value (1:5 extract)		8.4	7.9
Total N	%	0.056	0.15
Sand	%	71.8	86.9
Silt	%	15.7	7.6
Clay	%	12.4	5.6
Soil Moisture Content	bars	0.3	0.3
	% by weight	13.3	10.5
	bars	5.0	5.0
	% by weight	7.7	5.0
	bars	15.0	15.0
	% by weight	6.5	2.4
	bars	air dry	air dry
	% by weight	1.6	1.0

contact with the soil extract and the electrodes in the extract alone. The Kjeldahl digestion method was used to determine organic N.

The soil particle size analyses were run using the hydrometer method. Soil moisture content measurements were made with pressure membrane apparatus.

Data for the Parshall and Gardena soils were taken from the literature (Reichman et al., 1966) and appear in Table 2.

Incubation Study

Data for nitrification rates as a function of temperature, moisture content, $N_{NH_4}^+$ concentration, and pH were obtained from an incubation experiment involving the Panoche and desert soils. Initially, 25 g samples of each soil were treated with 400 $\mu\text{g/g}$ $N_{NH_4}^+$ and incubated at a temperature of 25°C and a moisture content of about 1/3 bar suction. The incubation chamber was humidified to control evaporation. This run was continued until a maximal population of nitrifiers was established in each soil as evidenced by the shape of the NO_2^- plus NO_3^- versus time curve. Incubation times used to insure establishment of the maximal populations ranged from two weeks with the Panoche soil to four weeks with the desert soil.

Remaining samples were then incubated in duplicate at temperatures of 15, 25, and 35°C, and at moisture contents

Table 2. Some Chemical and Physical Properties of the Parshall and Gardena Soils*

Parameter	Units	Parshall	Gardena
NH ₄ ⁺ -N	µg/g	15.0	26.4
NO ₃ ⁻ -N	µg/g	2.0	5.1
Total N	%	0.090	0.20
pH value (saturated paste)		6.6	7.2
Cation Exchange Capacity	meq/100g	17.9	24.2
Conductivity (saturation extract)	mmhos/cm	0.42	0.80
Soil Moisture Content	bars % by weight	saturation 28.7	saturation 41.6
	bars % by weight	0.2 15.0	0.2 20.0
	bars % by weight	1.0 9.0	1.0 13.4
	bars % by weight	5.0 6.8	5.0 9.8
	bars % by weight	15.0 5.8	15.0 8.2
	bars % by weight	50.0 4.5	50.0 6.4

*Data taken from Reichman et al. (1966)

ranging from about 1/3 to 15 bars suction in humidified incubation chambers.

Duplicate samples were removed from the incubation chambers at time intervals ranging from 10 to 20 days for a period of up to 60 days. Following centrifuging, the supernatant solutions from 1:6 water extracts of these samples were analyzed for $N_{NH_4}^+$, $N_{NO_2}^-$ plus $N_{NO_3}^-$, and pH. pH values were determined while the supernatant solutions were in contact with the soil particles. The N analyses were conducted by semi-micro steam distillation techniques with MgO followed by Devarda's alloy. Total $N_{NH_4}^+$ in each sample was calculated from soluble $N_{NH_4}^+$ using experimental curves for exchangeable versus soluble $N_{NH_4}^+$ measured at the 1:6 dilution. A listing of the experimental data collected in the incubation study appears in Appendix C.

Ammonium Exchange Study

This study was done to help assess the ability of a computer model previously developed (Dutt et al., 1972) to calculate the distribution between soluble and exchangeable $N_{NH_4}^+$ at equilibrium. Experimental values were determined for soluble and exchangeable $N_{NH_4}^+$ concentrations in equilibrated samples over a range of moisture contents. Data were collected for the Panoche and desert soils. $N_{NH_4}^+$ (400 $\mu\text{g/g}$) in the form of NH_4Cl dissolved in distilled water was applied to triplicate samples of the two soils. Sample size

ranged from 25 to 500 g soil. Extracts at each moisture content were obtained either by centrifuging or by extracting in pressure membrane apparatus. The extracts were then analyzed for $N_{NH_4}^+$ using steam distillation techniques and MgO. KCl extracts (1N) of similar samples contained 93 to 95% of the $N_{NH_4}^+$ applied to the two soils. The experimental results of the NH_4^+ exchange study are presented in Figure 2.

pH Study

pH data were collected in duplicate for the Panoche and desert soils treated with 400 $\mu\text{g/g}$ $N_{NH_4}^+$ in the form of NH_4Cl . The moisture contents of these determinations were 20, 30, 40, 60, 100, 200, and 400% by weight. The soil-water extracts were separated from the soil particles by centrifuging, and pH measurements were made on the supernatant solutions. The liquid remained in contact with the soil particles during the measurements.

A second set of similar pH determinations was made except that HCl was added to each sample to lower the pH. The same amount of HCl was applied to each sample, but the quantity added lowered the pH of the 400% extract by about 1 pH unit. In addition, Ca^{++} concentrations were determined in each of the supernatant solutions by the DCyTA method. The results of this two-part study appear later in the paper.

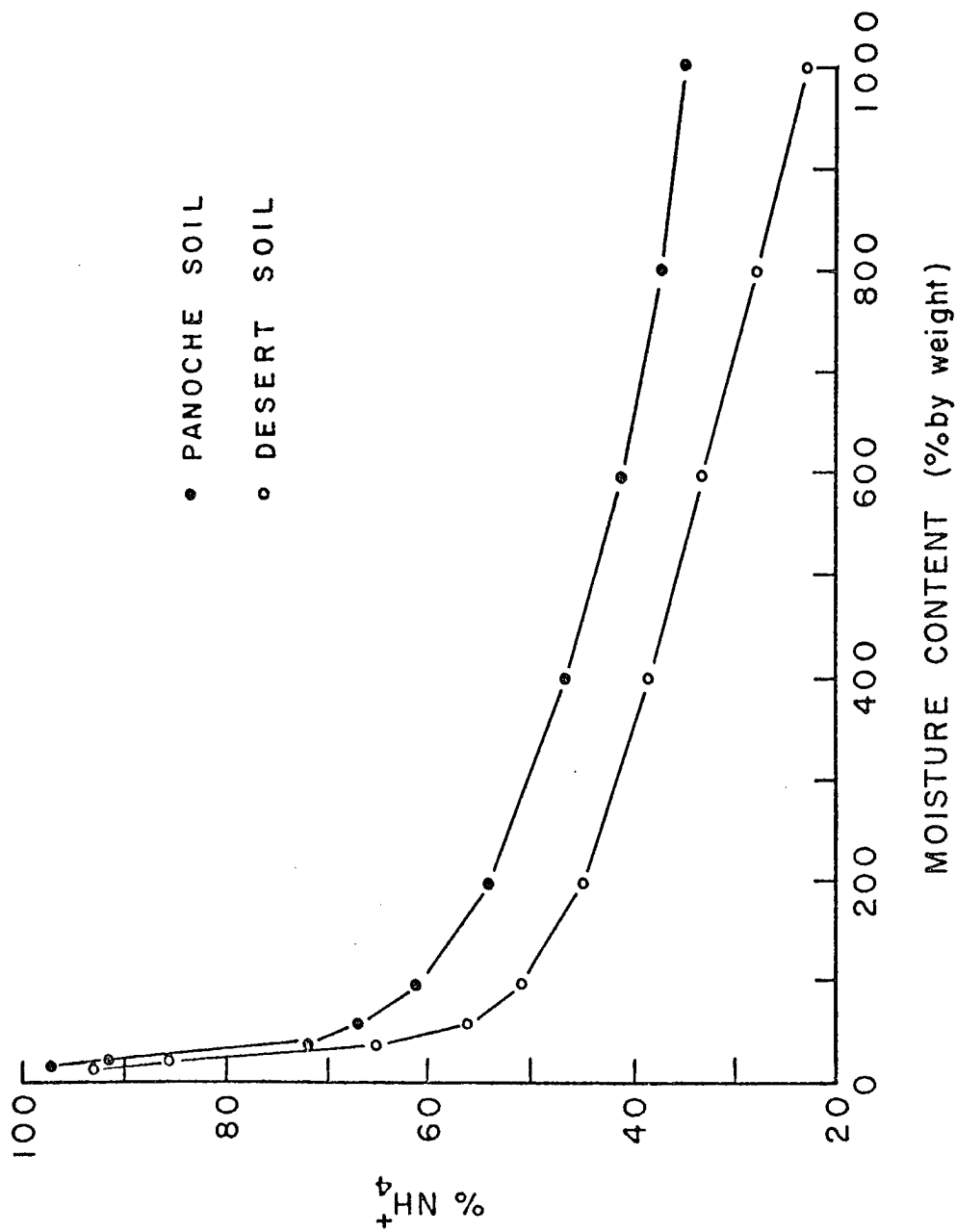


Figure 2. Percent of NH_4^+ on the Exchange Complex as a Function of Moisture Content.

RESULTS AND DISCUSSION

Ammonium and Oxygen

Previous researchers (e.g., Stojanovic and Alexander, 1957) have found that for enriched soils, the rate of NH_4^+ oxidation is independent of NH_4^+ and O_2 concentrated above respective saturation levels. This is probably caused by saturation of a limited number of active sites where the enzyme catalyzed reaction occurs. To test this hypothesis for NH_4^+ , correlation analyses were run on rates of reaction versus $N_{\text{NH}_4^+}$ concentrations and activities. Rates were included for the Panoche and desert soils, temperatures of 15, 25, and 35°C, and moisture contents ranging from about 1/3 to 15 bars. The results of these correlations appear in Tables 3 and 4. Activities were included because they were more likely to represent a true driving force in the reaction.

Note that in no case was there a significant correlation at the 0.05 level of significance even though various ways of expressing the $N_{\text{NH}_4^+}$ concentrations were used. The conclusions were made that this work confirmed the findings of previous researchers, and that the NH_4^+ concentrations and activities tested were in general above the critical saturation level for NH_4^+ oxidation to NO_2^- . A significant correlation might be expected for $N_{\text{NH}_4^+}$ concentrations and/or activities below the saturation level.

Table 3. Correlations for Nitrification Reaction Rates versus $N_{NH_4^+}$ Concentrations

Specie	Concentration Units	r*
**R-NH ₄ ⁺ -N	µg/g soil	-0.110
R-NH ₄ ⁺ -N	µg/ml water	-0.199
***S-NH ₄ ⁺ -N	µg/g soil	0.241
S-NH ₄ ⁺ -N	µg/ml water	0.0771
****T-NH ₄ ⁺ -N	µg/g soil	-0.0988
T-NH ₄ ⁺ -N	µg/ml water	-0.231

** R = exchangeable

*** S = soluble

**** T = total

* r must be at least 0.273 to be significant at the 0.05 level

Table 4. Correlations for Nitrification Reaction Rates versus $N_{NH_4^+}$ Activities

Specie	Concentration Units	r*
R-NH ₄ ⁺ -N	µg/g soil	-0.0947
R-NH ₄ ⁺ -N	µg/g ml water	-0.204
S-NH ₄ ⁺ -N	µg/g soil	0.255
S-NH ₄ ⁺ -N	µg/ml water	0.0997
T-NH ₄ ⁺ -N	µg/g soil	-0.0821
T-NH ₄ ⁺ -N	µg/ml water	-0.201

An $N_{\text{NH}_4^+}$ concentration of 1.1 ppm has been mentioned (e.g., Knowles, Downing, and Barrett, 1965) as a saturation level for NH_4^+ oxidation. However, since all exchangeable $N_{\text{NH}_4^+}$ concentrations encountered in the incubation study were above about 5.0 ppm, the only inference which could be made was that the saturation level probably was about 5.0 ppm or less.

Experimental curves for percent of $N_{\text{NH}_4^+}$ on the exchange complex at various moisture contents and 23°C appear previously in Figure 2. The concentration of total $N_{\text{NH}_4^+}$ present in each case was equal to the concentration initially established in the samples used in the incubation experiment. These data were used to verify a computer model developed by Dutt et al. (1972) with respect to the distribution of $N_{\text{NH}_4^+}$ between the soluble and exchangeable forms. The model appeared to yield results which agreed well with experiment below about 20 to 40 percent moisture content by weight, but deviated at higher moistures. Table 5 lists some experimental and calculated values for the Panoche and desert soils in the moisture range where reasonable agreement was obtained with experiment. The experimental $\text{NH}_4^+ - \text{Na}^+$ exchange constants used to obtain the calculated values in Table 5 were 0.025 and 0.005 for the Panoche and desert soils, respectively.

Since the moisture contents in this study and in most soils under field conditions generally fall within the

Table 5. Calculated and Observed Values for Percent of $N_{NH_4^+}$ on the Exchange Complex

Moisture Content (% by weight)	(% Exchangeable $N_{NH_4^+}$)			
	Panoche		Desert	
	(exp)	(calc)	(exp)	(calc)
40	72.0	71.1	65.3	30.5
20	91.5	90.0	86.8	84.1
9	96.9	95.4	—	89.3
7	—	98.3	93.4	92.3

range where reasonable agreement was obtained with experiment and because of the relatively high percentage of exchangeable $N_{NH_4^+}$ in this range, the computer model was utilized to calculate the distribution between soluble and exchangeable $N_{NH_4^+}$. Applications to problems such as sediment laden streams and lakes where the moisture contents are considerably higher would require modification of the NH_4^+ exchange portion of the model. Replacement of the $NH_4^+ - Na^+$ exchange reaction with $NH_4^+ - Ca^{++}$ exchange may improve the model in these moisture regions.

With respect to O_2 , the assumption was made that the oxygen concentrations remained above the saturation level for oxygen in the NH_4^+ oxidation process. No attempt was made to gather experimental data for oxygen concentrations. A saturation value of 0.25 ppm was selected for O_2 . This agrees with a number suggested by Boon and Laudelout (1962).

pH

Because hydrogen ion activity has been shown to be an important variable in the nitrification process, some method was needed to include pH in the rate model. pH values for soil-water extracts could have been applied directly. However, since pH varies with moisture content, a procedure was developed to approximate pH values at field moisture contents from soil-water extract pH. The assumption was made that the pH values calculated in this manner

were proportional to the microscopic pH values important at the active enzyme sites.

Dutt et al. (1972) made the assumption of constant CO₂ partial pressure at constant moisture content and applied the relationship

$$\frac{K_{sp} K_2}{K_3} = \frac{[Ca^{++}] [HCO_3^-]^2}{[H_2CO_3]} \quad (57)$$

where [] denotes the activity of the particular specie K_{sp}, K₂, and K₃ are equilibrium solubility and dissociation constants.

Combining equation (57) with the assumption of constant CO₂ partial pressure at constant moisture content yields

$$K' = [Ca^{++}] [HCO_3^-] = \frac{K_{sp} K_2 [H_2CO_3]}{K_3} \quad (58)$$

where K' is a constant at constant moisture content. Dutt et al. (1972) determined the relationship between K' and moisture content for several soils and combined these results to obtain the expression

$$\log K' = - 1.68 \log M - 4.46 \quad (59)$$

where M is moisture content (% by weight).

Rearrangement of equation (51) yields the expression

$$[H^+]^2 = \frac{K_1 K_1 K_3 P_{CO_2}}{K_{SP}} [Ca^{++}] \quad (60)$$

With the assumption of constant P_{CO_2} at constant moisture content, equation (60) may be written

$$[H^+]^2 = K'' [Ca^{++}] \quad (61)$$

and

$$K'' = \frac{K_1 K_2 K_3 P_{CO_2}}{K_{SP}} \quad (62)$$

where K'' is a constant at constant moisture.

Combining equations (58) and (62) leads to

$$K'' = K' \frac{K_3^2}{K_{SP}^2} \quad (63)$$

Finally, combining equations (61) and (63)

$$H^+ = \sqrt{K' \frac{K_3^2}{K_{SP}^2} [Ca^{++}]} \quad (64)$$

Experimental differences in K' are probably caused by changes in P_{CO_2} and hydrogen ion exchange.

To test the above theory, experimental values for pH were determined in soil-water extracts from the Panoche and desert soils. Extracts were included for a range of moisture contents from 400 to 20 percent by weight. The 1:5 extract analyses and other soil data (see Table 1) were used to calculate values for the slope and Y-intercept in equation (59) together with values for Ca^{++} activities and finally pH at the various moistures. Calculated versus measured pH values appear in Table 6.

Table 6. Calculated and Observed pH Values for Panoche and Desert Soils

Soil	% Moisture	pH	
		Calculated	Observed
Panoche	400	8.1	8.1
	200	7.9	7.9
	100	7.6	7.7
	60	7.4	7.6
	40	7.3	7.4
	30*	7.2	7.3
	20*	7.0	7.2
	Desert	400	8.0
200		7.7	7.7
100		7.5	7.6
60		7.3	7.5
40		7.1	7.2
30*		7.0	7.1
20*		6.9	7.0

*pH determined on supernatant solution out of contact with the soil.

Data pairing of these calculated and measured pH values yielded R values of 0.987 and 0.980 for the Panoche and desert soils, respectively.

The assumption was made that the agreement between experiment and theory shown by the data in Table 6 exists at moisture contents below 20%. It was not possible to obtain sufficient extract volumes below about 40% to allow pH readings where the extracts were in contact with the soil particles while the measuring electrodes were in the extracts alone.

Since the nitrification reaction generates H^+ , soil pH tends to become lower as the reaction progresses depending on the buffer capacity of the particular soil. A method was needed to allow calculation of soil pH without the necessity for new values for the slope and Y-intercept in equation (59) as the soil pH changed. As a first approximation, the assumption was made that for small changes in pH (e.g., one pH unit or less) the slope in equation (59) remained about constant. With this assumption, the Y-intercept could be calculated from experimental soil-water extract pH and the Ca^{++} activity in the same sample. Thus

$$INT = -SLOPE \log M - \log K' \quad (65)$$

where INT is the Y-intercept

SLOPE is the slope

M is the moisture content of the extract

K' is determined from extract pH and Ca^{++} activity.

To test this approach, experimental values for pH and Ca^{++} concentration were determined in soil-water extracts from the Panoche and desert soils treated with HCl and at various moisture contents. Using these data, the extract and soil data previously mentioned, and the above procedure, the values appearing in Table 7 were obtained.

Partition Functions

Before the data could be applied to calculate experimental values for ΔE_C partition functions had to be derived describing the motions of the various molecules and ions. Basically, partition functions were derived for O_2 , H^+ , NH_4^+ , NH_2OH , N_2O , and NO_2^- . Several combinations of these were used in addition to the ones for NH_2OH and N_2O to learn something of the structure of the activated complex. In addition, the O_2 , NH_4^+ , and H^+ partition functions were used directly in each of the models tested.

Partition Function for O_2

Recall from equation (27) that

$$q(\text{total}) = q_{\text{tran}} q_{\text{rot}} q_{\text{vib}} q_{\text{ele}}$$

q_{ele} was not needed because it was removed and included in ΔE_C (or ΔE_0). q_{tran} for O_2 was obtained by application of equation (36) for translational motion in three dimensions together with the mass of the O_2 molecule. Since O_2 is a diatomic molecule, equations (37) and (39) for rotational

Table 7. Calculated and Observed pH Values for Panoche and Desert Soils Treated with HCl

Soil	% Moisture	pH	
		Calculated	Measured
Panoche	400	7.1	7.1
	200	6.9	6.9
	100	6.6	6.7
	60	6.4	6.5
	40	6.3	6.5
	30*	6.2	6.3
	20*	6.0	6.2
Desert	400	7.0	7.0
	200	6.7	6.8
	100	6.5	6.6
	60	6.3	6.4
	40	6.1	6.2
	30*	6.0	6.1
	20*	5.9	6.0

*pH determined on supernatant solution out of contact with the soil.

and vibrational motion respectively, were applied to obtain the remaining q 's. The necessary temperatures and symmetry number (Hill, 1960) are given in Table 8. q_{O_2} the total partition function of O_2 is

$$q_{O_2} = V \left(\frac{2\pi M_{O_2} kT}{h^2} \right)^{3/2} T / (\sigma \theta_r) \exp[-\theta_v / (2T)] / [1 - \exp(-\theta_v / T)] \quad (66)$$

where M_{O_2} is the mass of the O_2 molecule.

Table 8. Data for Rotational and Vibrational Partition Functions and for O_2

Parameter	Value	Units
θ_r	2.07	$^{\circ}K$
θ_v	2230.	$^{\circ}K$
Symmetry Number	2.	_____

Partition Function for H^+

This function is relatively simple since monatomic species do not have rotational and vibrational degrees of freedom. Derivation consisted of applying equation (36) together with the mass of the hydrogen ion. Thus

$$q_{H^+} = V \left(\frac{2\pi M_H kT}{h^2} \right)^{3/2} \quad (67)$$

where M_{H^+} is the mass of the hydrogen ion.

Partition Function for NH_4^+

Derivation of the total partition function for the polyatomic NH_4^+ ion consisted of applying equations (36), (38), and (40), together with other information. There are few experimental data available on the specific rotational and vibrational temperatures for the NH_4^+ ion. However, experimental work has been done on a molecule with a very similar configuration, CH_4 (methane). Both CH_4 and NH_4^+ have a tetrahedral (spherical top) shape. Of course some differences do exist due to different bond lengths and the presence of the positive charge. The partition function, however, is determined primarily by the special configuration. Therefore, the assumption was made that methane data have application here.

The rotational temperature for methane is the same for all three moments of inertia and equal to 7.47°K . The symmetry number is 12. The vibrational temperatures for the 9 vibrational modes (3.5 - 6) were deduced from spectral data (e.g., Sadtler Research Laboratories, 1967). The modes occurring at about 3.35 microns are known to possess 4-fold degeneracy due to stretching of each hydrogen bond. In addition, the mode at about 7.65 microns was assumed to possess 2-fold degeneracy due to the nature of the peaks in this region. The wave lengths selected appear in Table 9.

Table 9. Wave Lengths of Vibrational Modes for NH_4^+

Wave Length (microns)	Assumed Degeneracy	Totals
2.38	None	1
3.35	4-fold	4
7.40	None	1
7.65	2-fold	2
15.00	None	<u>1</u>
		Total 9

The wave length was converted to frequency by

$$\nu = C/\lambda \quad (68)$$

where ν is frequency

λ is wave length

C is the spread of light.

The final form of $q_{\text{NH}_4^+}$ can be written

$$q_{\text{NH}_4^+} = V \left(\frac{2\pi M_{\text{NH}_4^+} kT}{h^2} \right)^{3/2} \cdot \frac{\sqrt{\pi}}{\sigma} \left(\frac{T^3}{\theta_A \theta_C \theta_C} \right)^{1/2} \prod_{\nu_i=1}^9 \frac{\exp[-\theta_{\nu_i}/(2T)]}{[1-\exp(-\theta_{\nu_i}/T)]} \quad (69)$$

where $M_{\text{NH}_4^+}$ is the mass of NH_4^+

i varies from 1 to 9.

Partition Function for NH_2OH

The translational and rotational partition functions for NH_2OH have the same basic form as for any polyatomic molecule or ion. The mass of NH_2OH was included in the translational part while a symmetry number of 3 was used in the rotational function. Since the rotational moments for NH_2OH are difficult to determine, two rotational temperatures were assumed to be approximated by the rotational temperatures used for NH_4^+ , and the third was assumed equal to the rotational temperature for O_2 . Here the basic assumptions were that the molecule has a configuration similar to a symmetrical top and the same symmetry number as NH_3 .

Since NH_2OH contains five nuclei, the total number of vibrational energy modes would be 8 (not 9) because one mode (degree of freedom) is taken up by the reaction coordinate. The 8 vibrational wave lengths were deduced from the IR spectra for $\text{NH}_2\text{OH}\cdot\text{HCl}$ and HCl . The HCl spectrum was used to eliminate the HCl contribution from the $\text{NH}_2\text{OH}\cdot\text{HCl}$ spectrum at about 3.5 microns. Remaining peaks were assumed to be due to NH_2OH . A summary of the wave lengths for the 8 vibrational modes appears in Table 10. The total partition function ($q_{\text{NH}_2\text{OH}}$) for NH_2OH is

$$q_{\text{NH}_2\text{OH}} = V \left(\frac{2\pi M_{\text{NH}_2\text{OH}} kT}{h^2} \right)^{3/2} \frac{\sqrt{\pi}}{\sigma} \left(\frac{T^3}{\theta_A \theta_C \theta_C} \right)^{1/2} \quad (70)$$

$$\prod_{v_i=1}^8 \frac{\exp[-\theta_{v_i}/(2T)]}{[1-\exp(-\theta_{v_i}/T)]}$$

where $M_{\text{NH}_2\text{OH}}$ is the mass of NH_2OH

i varies from 1 to 8.

Partition Function for N_2O

N_2O is a linear molecule with the structure NNO . This means the symmetry number is equal to 1. The rotational temperature is about 2.42°K , and the 4 vibrational temperatures are 850, 850, 1840, and 3200°K . The usual translational partition function was applied (with N_2O mass)

Table 10. Wave Lengths of Vibrational Modes for NH_2OH

Wave Lengths (microns)	Assumed Degeneracy	Totals
3.4	None	1
4.4	None	1
5.5	None	1
6.4	None	1
6.8	None	1
7.2	None	1
8.4	None	1
8.7	None	1
		<hr/>
	Total	8

together with the rotational function for diatomic molecules (always used for linear molecules). Finally, the vibrational partition function for nonlinear molecules was used with one degree of vibrational freedom removed for the reaction coordinate. The total partition function ($q_{\text{N}_2\text{O}}$) is

$$q_{\text{N}_2\text{O}} = V \left(\frac{2\pi M_{\text{N}_2\text{O}} kT}{h^2} \right)^{3/2} \cdot T / (\sigma \theta_r) \cdot \quad (71)$$

$$\prod_{v_i=1}^3 \exp[-\theta_{v_i}/(2T)] / [1 - \exp(-\theta_{v_i}/T)]$$

Partition Function for NO_2^-

The nitrite ion (NO_2^-) has a v-shaped structure similar to H_2O . The N-O bond length is 1.24 \AA and the bond angle is 115° , Jolly (1964). This may be compared with a H-O bond length of 0.96 \AA and an angle of 104° for H_2O . Because of these similarities and the availability of the partition function for water (e.g., Hill, 1960), the assumption was made that $q_{\text{NO}_2^-}$ can be approximated by application of $q_{\text{H}_2\text{O}}$. Since $q_{\text{NO}_2^-}$ was used as a partition function for an activated complex, one vibrational degree of freedom was omitted to allow for the reaction coordinate. Values used for the various parameters contained in q_{rot} and q_{vib} for this polyatomic ion are presented in Table 11.

Table 11. Data for Rotational and Vibrational Partition Functions for NO_2^-

Parameter	Value	Units
θ_A	$3.94 \cdot 10^{-39}$	$^\circ\text{K}$
θ_B rotational	$2.10 \cdot 10^{-39}$	$^\circ\text{K}$
θ_C	$1.37 \cdot 10^1$	$^\circ\text{K}$
θ_{v_1} vibrational	$5.28 \cdot 10^3$	$^\circ\text{K}$
θ_{v_2}	$5.43 \cdot 10^3$	$^\circ\text{K}$
σ	2	—

The total partition function ($q_{\text{NO}_2^-}$) may be written

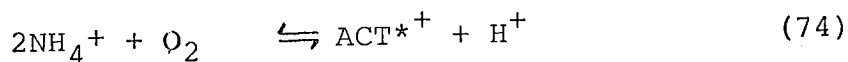
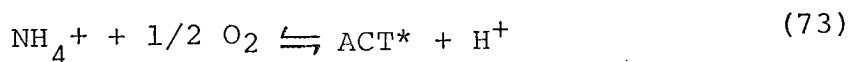
$$q_{\text{NO}_2^-} = V \left(\frac{2\pi M_{\text{NO}_2^-} kT}{h^2} \right)^{3/2} \cdot \frac{\sqrt{\pi}}{\sigma} \left(\frac{T^3}{\theta_A \theta_B \theta_C} \right)^{1/2} \quad (72)$$

$$\prod_{v_i=1}^2 \exp[-\theta_{v_i}/(2T)] / [1 - \exp(-\theta_{v_i}/T)]$$

where $M_{\text{NO}_2^-}$ is the mass of NO_2^-
 i varies from 1 to 2.

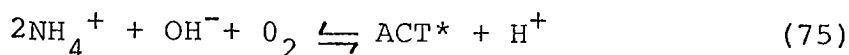
Comparison of Equation Forms and Activated Complexes

To obtain some insight into the mechanisms governing the NH_4^+ oxidation process, various equation forms and activated complexes were applied to the experimental rate data from the Panoche and desert soils. Two promising equation forms for the equilibrium between the reactants and the activated complex are



If ACT^* in equation (73) is replaced with NH_2OH , we have the familiar equation for the formation of the NH_2OH intermediate. Equation (74) was selected because it initially showed promising agreement with the experimental results.

Other equations were tried such as



and equations that were even higher order with respect to NH_4^+ and O_2 but lacked the OH^- . These equations, however, did not fit experiment as well as equations (73) and (74).

Using equations (73) and (74), various activated complexes were applied to the experimental data. Both equations should have, in theory, yielded a linear relationship for the observed activation energy versus ionic strength. For example, equation (74) yields the following expression when concentrations in equation (35) are replaced with activities

$$\text{RATE} = \frac{kT}{h} [q's] \frac{\gamma_{\text{NH}_4^+}^2 (\text{NH}_4^+)^2 \gamma_{\text{O}_2} (\text{O}_2)}{\gamma_{\text{ACT}^*} \gamma_{\text{H}^+} (\text{H}^+)} \quad (76)$$

$$\exp(-\Delta\epsilon_c/kT)$$

where $q's$ denotes the partition functions in equation (35)

() stands for concentration

γ is the activity coefficient.

Equation (76) reduces to

$$\text{RATE} = \frac{kT}{h} [q's] \frac{(\text{NH}_4^+)^2 (\text{O}_2) \exp(K_m \mu)}{(\text{H}^+)} \exp(-\Delta\epsilon_c/kT) \quad (77)$$

when combined with equation (46). Also

$$\text{RATE} = kT/h [q's] \frac{(\text{NH}_4^+)^2 (\text{O}_2)}{(\text{H}^+)} \exp(-\Delta\epsilon_m/kT) \quad (78)$$

where $\Delta\epsilon_m$ is the measured activation energy per molecule at the ionic strength of the solution.

At this point, equations (77) and (78) may be equated to give

$$\exp(\bar{K}_m\mu) \exp(-\Delta\epsilon_c/kT) = \exp(-\Delta\epsilon_m/kT) \quad (79)$$

which reduces to

$$\Delta\epsilon_m = \Delta\epsilon_c - kT \bar{K}_m\mu \quad (80)$$

The temperature effect can be ignored over a narrow temperature range (e.g., the range encountered in this study) to yield

$$\Delta\epsilon_m = \Delta\epsilon_c - K_s\mu \quad (81)$$

where K_s is a constant

$\Delta\epsilon_c$ is the activation energy per molecule at infinite dilution.

Equation (81) may be rewritten as

$$\Delta E_m = \Delta E_c - \bar{K}_s\mu \quad (82)$$

where ΔE_m and ΔE_c are activation energies expressed in Kcal/mole

\bar{K}_s is a constant.

Any deviation from the linearity predicted by equation (82) indicated failure of the theory to fit experiment or experimental errors in the data. Since the same data set (Parshall and Gardena soils) was used for all combinations of equations and activated complexes, any changes in the goodness of fit of a regression of ΔE_m on μ indicated changes in agreement between theory and experiment. A summary of the activated complexes tried for each equation form and the corresponding statistics appears in Tables 12 through 15. In some cases partition functions for different activated complexes were multiplied together to simulate interactions between these functions. These cases are denoted by a dot between q subscript parts; each basic partition function being on either side.

In general the R values and F ratios are higher for the application of equation (74) than for equation (73). Also, equation (74) yielded lower s_y and s_b values. Equation (74) appears to more nearly model the experimental data used here for the Panoche and desert soils. This means that a reaction between NH_4^+ and O_2 to stoichiometrically form NH_2OH probably does not represent the equation form for the equilibrium between the reactants and the activated complex for NH_4^+ oxidation to NO_2^- . The actual form of the equilibrium equation probably is closer to that represented by equation (74).

Table 12. Partition Functions and Statistical Data for Equation (73) and Panoche Soil

Q_{ACT}^*	R	s_y^*	s_b^{**}	F ratio
Q_{NH_2OH}	0.794	1.01	0.208	32.5
$Q_{NH_4^+}$	0.802	0.973	2.01	34.4
$Q_{NH_4^+ \cdot NH_2OH}$	0.723	1.32	2.73	20.8
$Q_{O_2 \cdot NH_2OH}$	0.721	1.33	2.75	20.6
Q_{N_2O}	0.797	0.996	2.06	33.1
$Q_{N_2O \cdot NH_2OH}$	0.718	1.34	2.77	20.2
$Q_{N_2O \cdot NH_4^+}$	0.725	1.31	2.70	21.1
$Q_{NO_2^-}$	0.580	2.17	4.49	9.63
$Q_{NO_2^- \cdot NH_2OH}$	0.538	2.54	5.25	7.72
$Q_{NO_2^- \cdot N_2O}$	0.539	2.53	5.22	7.77

* s_y is the standard deviation of the dependent variable.

** s_b is the standard deviation of the slope.

Note: The critical values at the 0.05 level are 0.433 and 4.38 for the R and F ratios, respectively.

Table 13. Partition Functions and Statistical Data for Equation (74) and Panoche Soil

q_{ACT}^*	R	s_y	s_b	F ratio
q_{NH_2OH}	0.941	0.550	1.14	117
$q_{NH_4^+}$	0.929	0.545	0.113	119
$q_{NH_4^+ \cdot NH_2OH}$	0.847	0.797	1.65	48.5
$q_{O_2 \cdot NH_2OH}$	0.869	0.819	0.169	58.5
q_{N_2O}	0.926	0.558	0.115	114
$q_{N_2O \cdot NH_2OH}$	0.914	0.538	1.11	95.8
$q_{N_2O \cdot NH_4^+}$	0.873	0.800	0.165	61.0
$q_{NO_2^-}$	0.665	1.62	3.34	15.0
$q_{NO_2^- \cdot NH_2OH}$	0.607	1.98	4.09	11.1
$q_{NO_2^- \cdot N_2O}$	0.608	1.97	4.06	11.2

Table 14. Partition Functions and Statistical Data for Equation (73) and Desert Soil

q_{ACT}^*	R	s_y	s_b	F ratio
q_{NH_2OH}	0.475	0.596	0.225	8.19
$q_{NH_4^+}$	0.466	0.564	0.213	7.77
$q_{NH_4^+ \cdot NH_2OH}$	0.522	0.897	0.339	10.5
$q_{O_2 \cdot NH_2OH}$	0.522	0.907	0.343	10.5
q_{N_2O}	0.472	0.585	0.221	8.06
$q_{N_2O \cdot NH_2OH}$	0.523	0.919	0.347	10.6
$q_{N_2O \cdot NH_4^+}$	0.521	0.885	0.334	10.4
$q_{NO_2^-}$	0.550	1.74	0.657	12.1
$q_{NO_2^- \cdot NH_2OH}$	0.554	2.10	0.793	12.4
$q_{NO_2^- \cdot N_2O}$	0.554	2.09	0.789	12.4

Note: The critical values at the 0.05 level are 0.361 and 4.20 for the R and F ratios, respectively.

Table 15. Partition Functions and Statistical Data for Equation (74) and Desert Soil

q_{ACT}^*	R	s_y	s_b	F ratio
q_{NH_2OH}	0.686	0.295	0.112	21.4
$q_{NH_4^+}$	0.648	0.296	0.112	20.3
$q_{NH_4^+ \cdot NH_2OH}$	0.369	0.409	0.155	4.39
$q_{O_2 \cdot NH_2OH}$	0.753	0.447	0.169	36.6
q_{N_2O}	0.675	0.294	0.111	23.4
$q_{N_2O \cdot NH_2OH}$	0.677	0.294	0.111	1.35
$q_{N_2O \cdot NH_4^+}$	0.521	0.885	0.334	10.4
$q_{NO_2^-}$	0.538	1.19	0.449	11.4
$q_{NO_2^- \cdot NH_2OH}$	0.547	1.55	0.584	12.0
$q_{NO_2^- \cdot N_2O}$	0.547	1.53	0.579	11.9

The determination of the exact structure of the activated complex or the significant part(s) of the complex is an extremely difficult task. However, some insight may be gained by examining the values for the statistical parameters calculated for each hypothetical activated complex tried. Relatively poor agreement with experiment was obtained in the cases of the NO_2^- and NO_2^- related complexes. Relative agreement with experiment occurred when application was made of theoretical models containing NH_4^+ , NH_2OH , and related activated complexes.

The activated complex involved in NH_4^+ oxidation to NO_2^- probably is closer in structure to NH_4^+ and/or NH_2OH than to NO_2^- . The true activated complex probably has a structure somewhere intermediate between NH_4^+ and NH_2OH . Future investigations centered around this type intermediate could reveal more structural details.

The Rate Model

Although certain other activated complexes showed promise, $q_{\text{NH}_2\text{OH}}$ and equation (74) were selected for the rate model. $q_{\text{NH}_2\text{OH}}$ was selected because NH_2OH is a known intermediate in the nitrification pathway and because it yielded promising values for the statistical parameters evaluated in the regression analyses. Equation (74) was selected because of its consistently closer agreement with experiment for the various activated complexes. These

parameters were combined into the previously discussed rate theory to form the final rate model.

Basic Assumptions

To insure best use of the rate model, the basic assumptions inherent in it are listed below.

1. $q_{\text{NH}_2\text{OH}}$ is a satisfactory approximation of the true activated complex or active part of that complex.
2. Equation (74) represents a satisfactory approximation of the equilibrium reaction between the reactants and the activated complex.
3. The population of Nitrosomonas is maximal and constant.
4. Nitrobacter is uninhibited, or if inhibited, NH_4^+ oxidation to NO_2^- is modeled. In the first case, the model applies to the entire nitrification process.
5. Nitrosomonas is not inhibited by factors not considered in the model (e.g., sufficient phosphorus and carbon are present.)
6. Any missing part(s) of the activated complex either contribute insignificantly to the rate process or contribute in a constant manner.
7. The enzyme system and activated complex are unaffected by environmental factors such as temperature, moisture content, and pH.

8. A linear relationship (as predicted by theory) exists between ΔE_m and μ .
9. The soil is calcareous.
10. The NH_4^+ , O_2 , and H^+ activities used in the model are proportional to the localized activities at the active sites.
11. H^+ remains below the saturation level (if one exists at measurable reaction rates).
12. Activities of saturation values vary with ionic strength while concentrations are independent of the same.
13. The saturation concentration for $\text{N}_{\text{NH}_4^+}$ is $1.0 \mu\text{g/g}$ soil.
14. The saturation concentration for O_2 is $0.25 \mu\text{g/ml}$ water.
15. Saturation values are independent of temperature.
16. The assumptions used to derive the partition functions used in the model are valid.
17. The reaction rate is unaffected by changes in hydrostatic pressure.
18. The reaction rate is unaffected by changes in dielectric constant.

Computer Program

Since many of the computations involved in the rate model are tedious and time consuming, the rate function was

programmed in FORTRAN IV computer language for C.D.C. 6000 series machines. The calculations involved in the development of the rate model were similarly programmed. A block diagram of the final nitrification rate subroutine appears in Figure 3. A complete FORTRAN listing of this subroutine and the program used to develop the rate model appears in Appendices A and B, respectively.

Application of Nitrification Rate Model to Panoche and Desert Soils

Plots of measured activation energy (ΔE_m) versus ionic strength for the Panoche and desert soils appear in Figure 4. These data were obtained using the rate model just described. Neither the Y-intercepts nor the slopes of the best-fit regression lines through these data sets agree closely. Still different Y-intercepts and slopes were obtained for the Northern Plains soils used in the verification procedure described later. Intercept differences may reflect differences in maximal population sizes. Soils with different size populations of Nitrosomonas would be expected to exhibit different values for the activation energy at infinite dilution (ΔE_C).

Differences in slope are more difficult to resolve, but may reflect variations in local populations of nitrifiers. For example, Nitrosomonas subspecies from desert regions might be expected to be more tolerant of lower moisture contents and resulting higher ionic strengths. This appears to

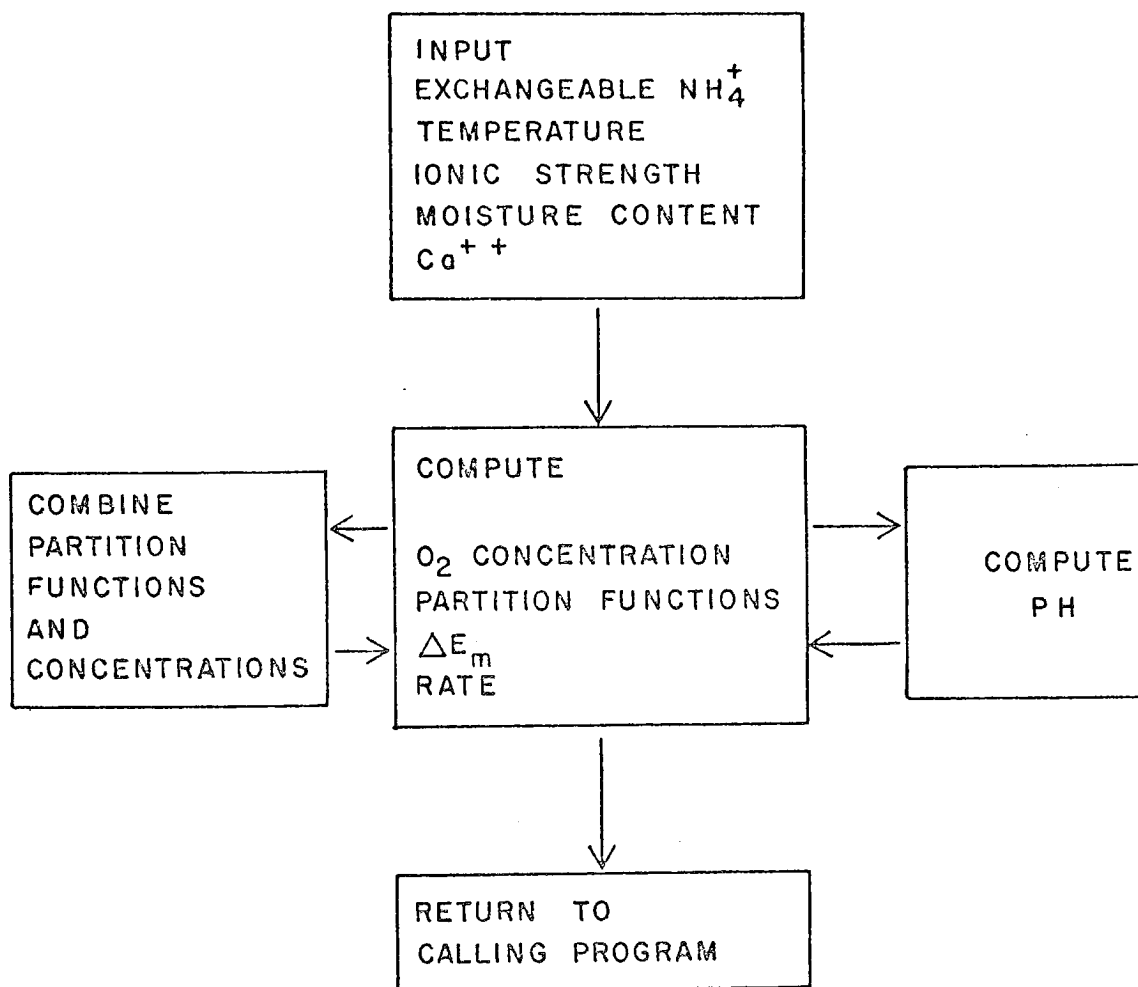


Figure 3. Block Diagram of Computerized Rate Subroutine.

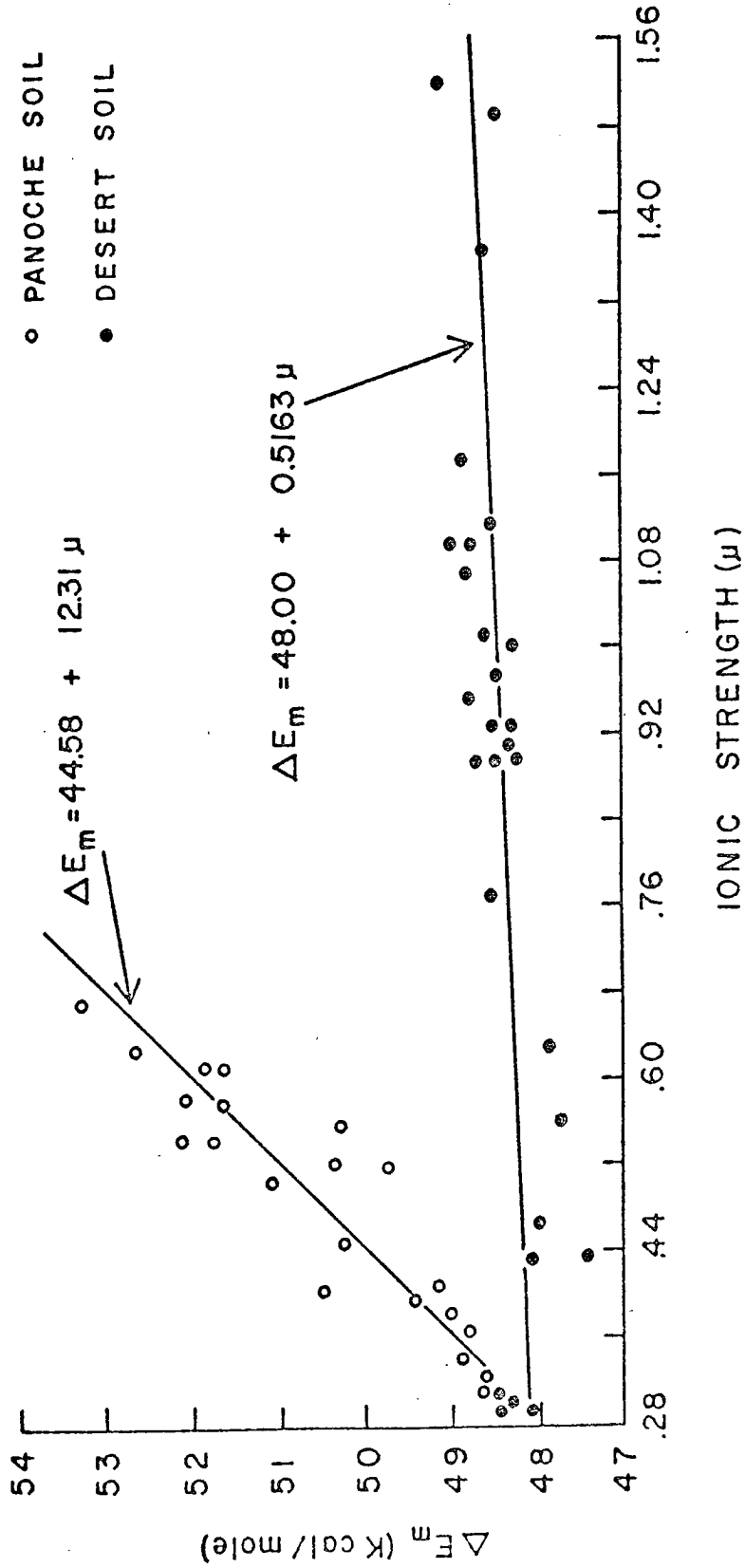


Figure 4. Relationship of Activation Energy to Ionic Strength for Panoche and Desert Soils.

be the case with the native desert soil, since it has a lower slope than the Panoche soil from California. Also, various other researches (e.g., Quastel and Scholefield, 1951) have noted that populations of nitrifiers do not all display the same nitrifying capacities. Since Nitrosomonas must depend on NH_4^+ oxidation for its sole energy source and therefore its survival, it is easy to imagine the strong adaptive influences of environmental conditions on the process.

Even with local variations, however, Nitrosomonas appears to display characteristics which can be described by the theory previously discussed. A linear relationship between ΔE_m and μ appears to hold regardless of local population variations.

To gain some appreciation for the predictive capabilities of the rate model as applied to the Panoche and desert soils, rates were computed based on the input data used to develop the model. Although the model would be expected to fit this data with a reasonable degree of accuracy, a comparison of observed and calculated rates could indicate the potential of the model. The resulting statistics from a data pairing of 51 pairs of nitrification rate data from the Panoche and desert soils appears in Table 16.

Table 16. Statistical Data from Pairing Calculated and Observed Rates for the Panoche and Desert Soils

Parameter	Value*
R	0.956
s_y	1.04
Y-intercept	-0.438
b	1.19
F ratio	540.

*Rates expressed in ppm/day

Additional Verification of Nitrification Rate Model

To further verify the theoretical rate model, data for two Northern Plains soils were taken from the literature (Reichman et al., 1966). Nitrification rate data were available for a temperature of 28°C and moisture contents ranging from about 0.2 to 50 bars suction. Assuming the previously determined linear relationship between ΔE_m and μ , the following regression equations were derived for the Parshall and Gardena soils

$$\text{(Parshall)} \quad \Delta E_m = 50.8 + 48.7\mu \quad (83)$$

$$\text{(Gardena)} \quad \Delta E_m = 49.8 + 8.57\mu \quad (84)$$

where the Y-intercept (ΔE_c) is the activation energy at infinite dilution.

Ionic strength was determined using the Dutt Model (e.g., Dutt et al., 1972).

Equations (83) and (84) were used in the theoretical rate model together with the other necessary data to calculate predicted nitrification rates and $N_{NO_3^-}$ concentrations with time. A summary of calculated and observed nitrification rates appears in Table 17. Data pairing of the rates presented in Table 18.

Table 17. Calculated and Observed Nitrification Rates for the Parshall and Gardena Soils

Soil	Rate (ppm/10 days)	
	Observed	Calculated
Parshall	3.45	5.43
	3.39	4.82
	3.26	3.52
	3.00	3.02
	10.1	9.42
	8.71	7.25
	5.92	3.31
	0.324	0.392
	15.7	20.9
	13.7	14.6
	9.63	7.76
	1.51	1.03
	Gardena	16.3
13.4		11.4
7.57		6.79
14.4		15.7
12.3		13.0
8.09		10.2
20.9		22.5
17.2		19.5
9.69		12.9
30.5		27.6
25.1		21.0
14.3	12.8	

Table 18. Statistical Data from Pairing Calculated and Observed Nitrification Rates for Parshall and Gardena Soils

Soil	Parameter	Value
Parshall	R	0.944
	s_y	2.066
	b	1.13
	Y-intercept	-0.629
	F ratio	81.5
Gardena	R	0.940
	s_y	2.14
	b	0.812
	Y-intercept	2.72
	F ratio	74.4

Plots of calculated and observed $N_{NO_3^-}$ concentrations as a function of moisture content appear in Figures 5 through 9. These data were based on the rates in Table 17.

The following assumptions and approximations were used in making the verification runs on the Parshall and Gardena soils.

1. The assumptions already mentioned with respect to the model were assumed to hold in this case.
2. The assumption was made that NO_2^- oxidation is faster than NH_4^+ oxidation.
3. In calculating the distribution of NH_4^+ between soluble and exchangeable forms, the $NH_4^+ - Na^+$ exchange constant was set equal to 0.22; a mean value for several soils and used in the current version of the model developed by Dutt, Shaffer, and Moore (1972).
4. The slope of equation (59) was set equal to the best-fit value of 1.68 determined by Dutt et al. (1972). The Y-intercept values in the same equation were determined from experimental and calculated data using the method previously discussed.
5. Additional data for the soil extract analyses needed to approximate ionic strengths and partition the total $N_{NH_4^+}$ into exchangeable and soluble fractions were obtained from the data of Reichman et al.

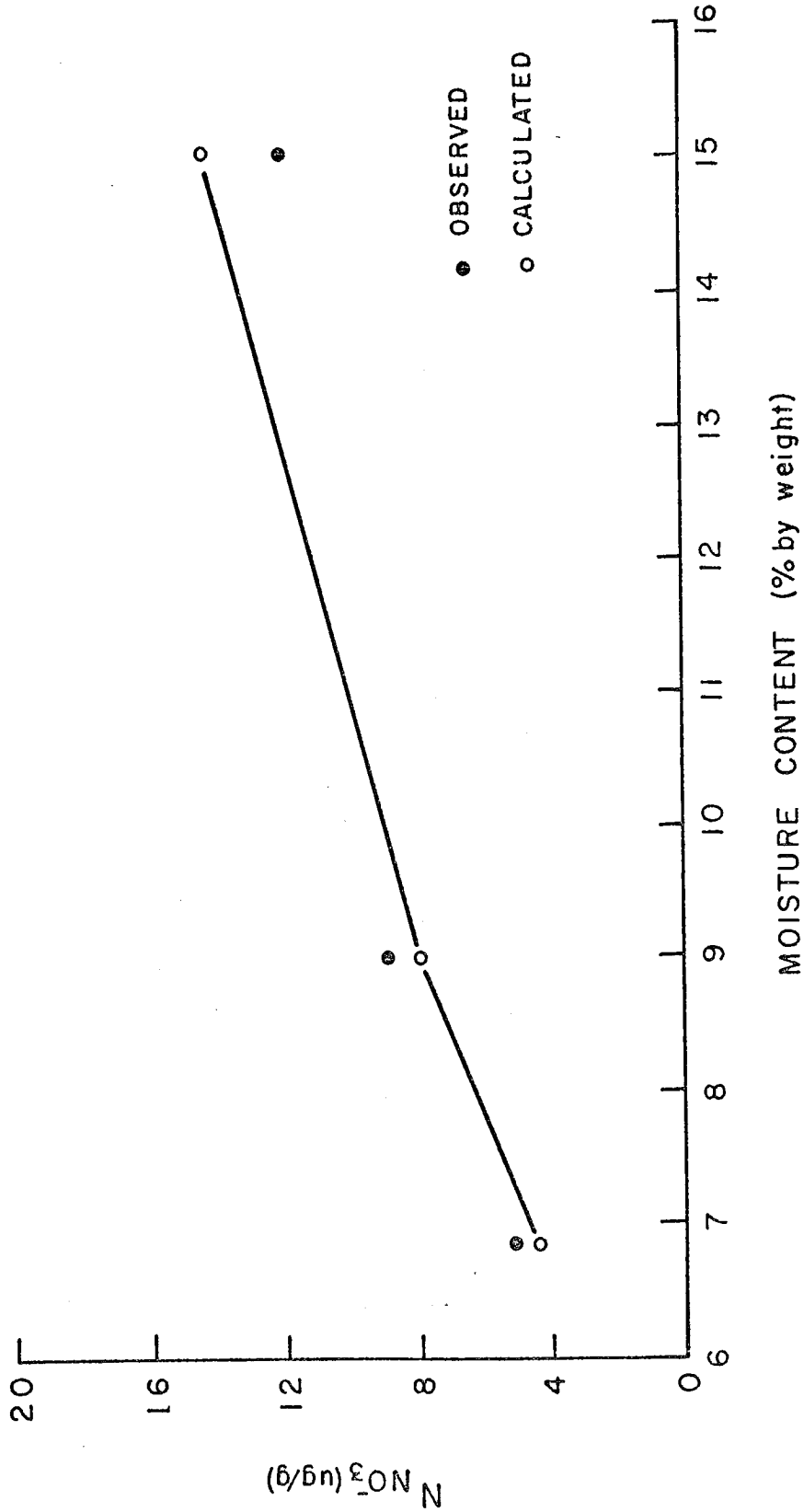


Figure 5. Calculated and Observed Rate Data for Parshall Soil at Various Moistures after 10 days incubation.

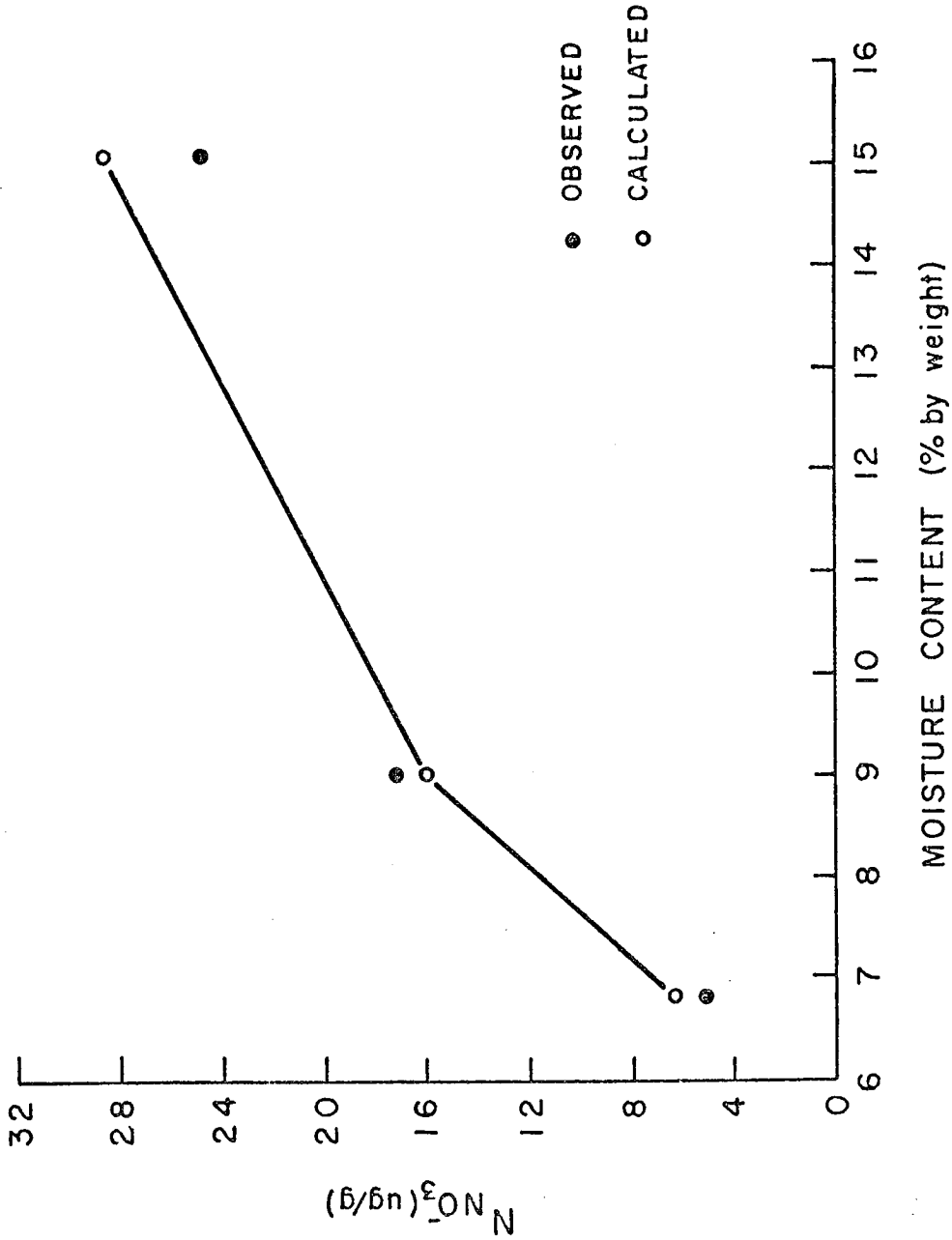


Figure 6. Calculated and Observed Rate Data for Parshall Soil at Various Moistures after 20 days Incubation.

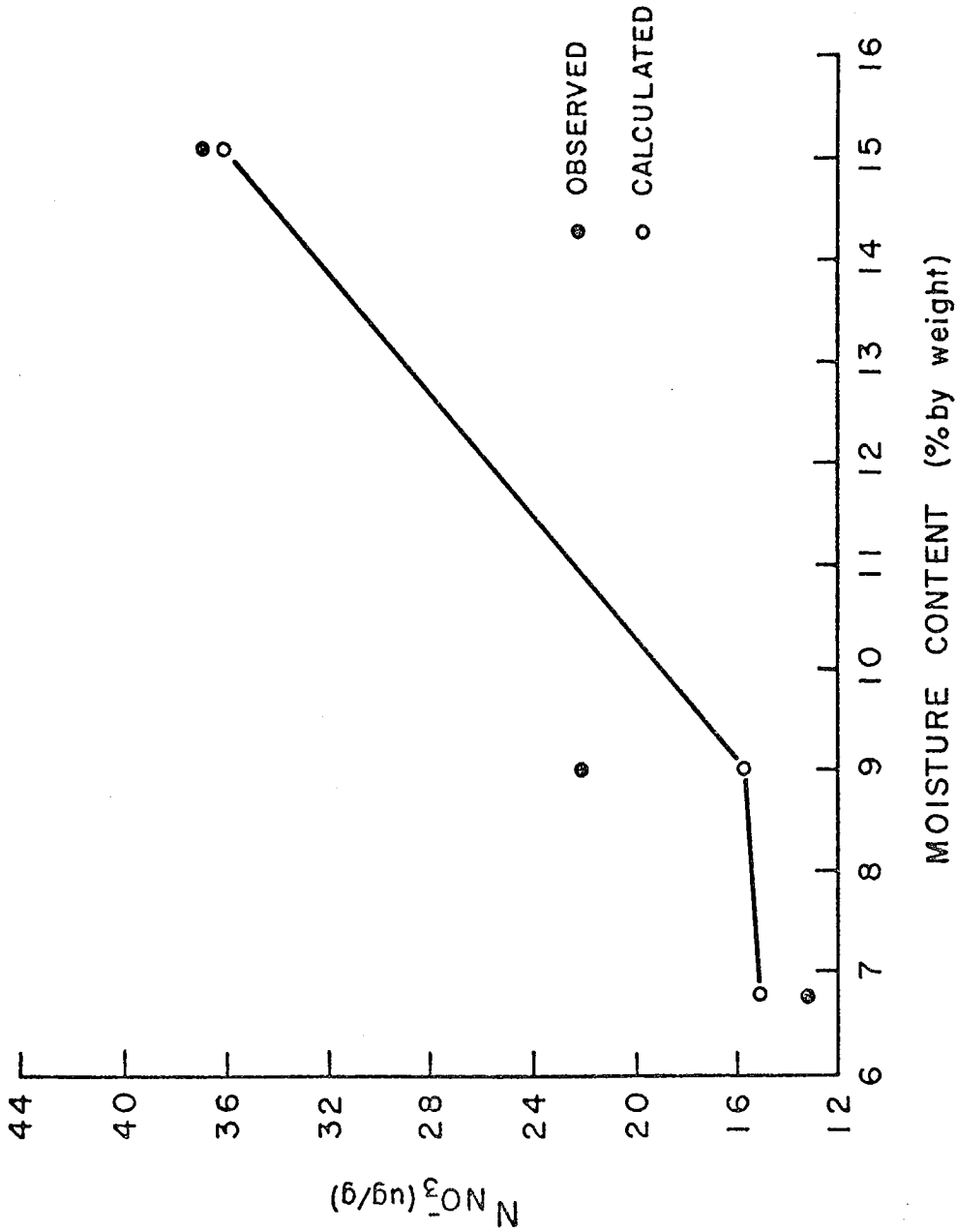


Figure 7. Calculated and Observed Rate Data for Parshall Soil at Various Moistures after 40 days Incubation.

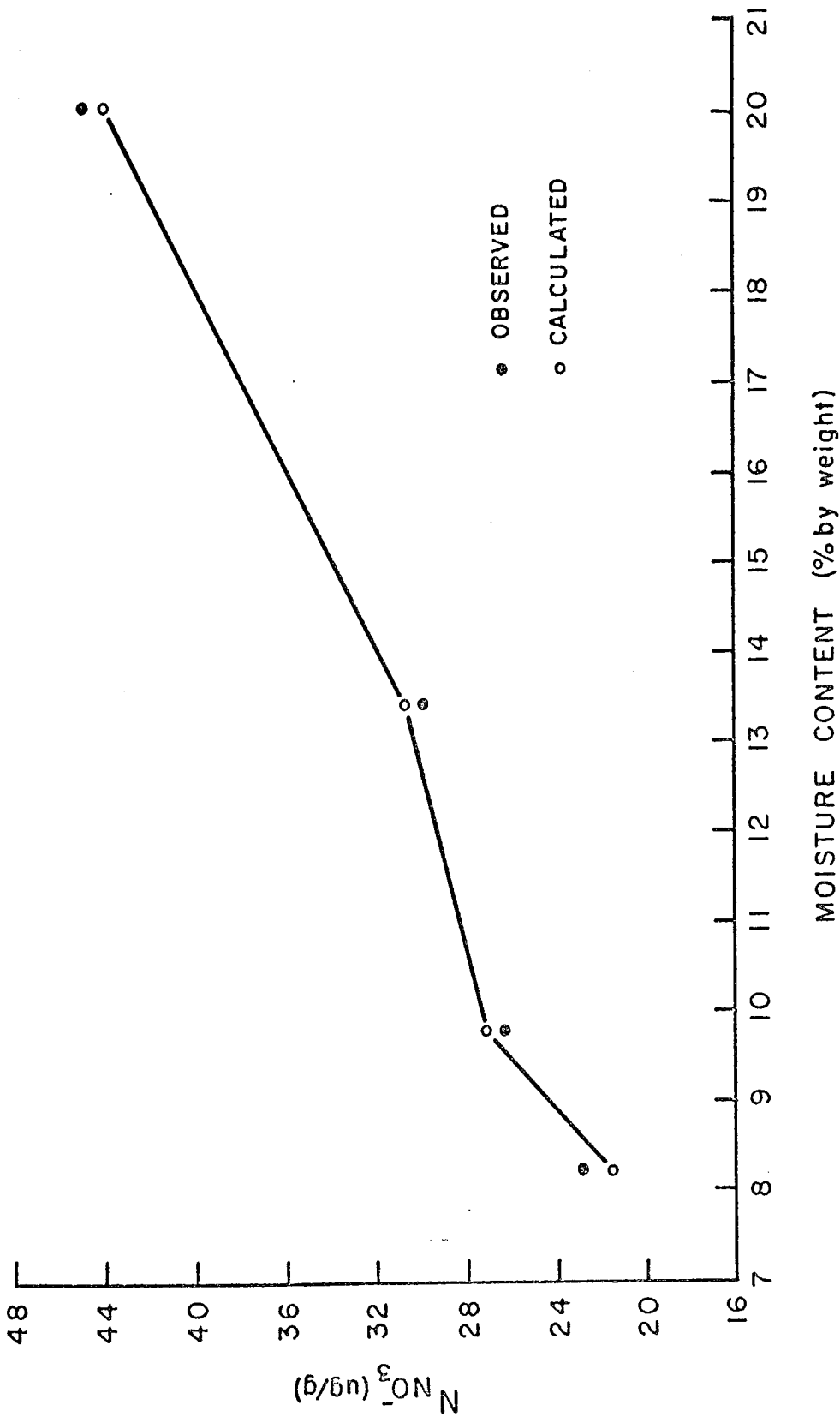


Figure 8. Calculated and Observed Rate Data for Gardena Soil at Various Moistures after 10 days Incubation.

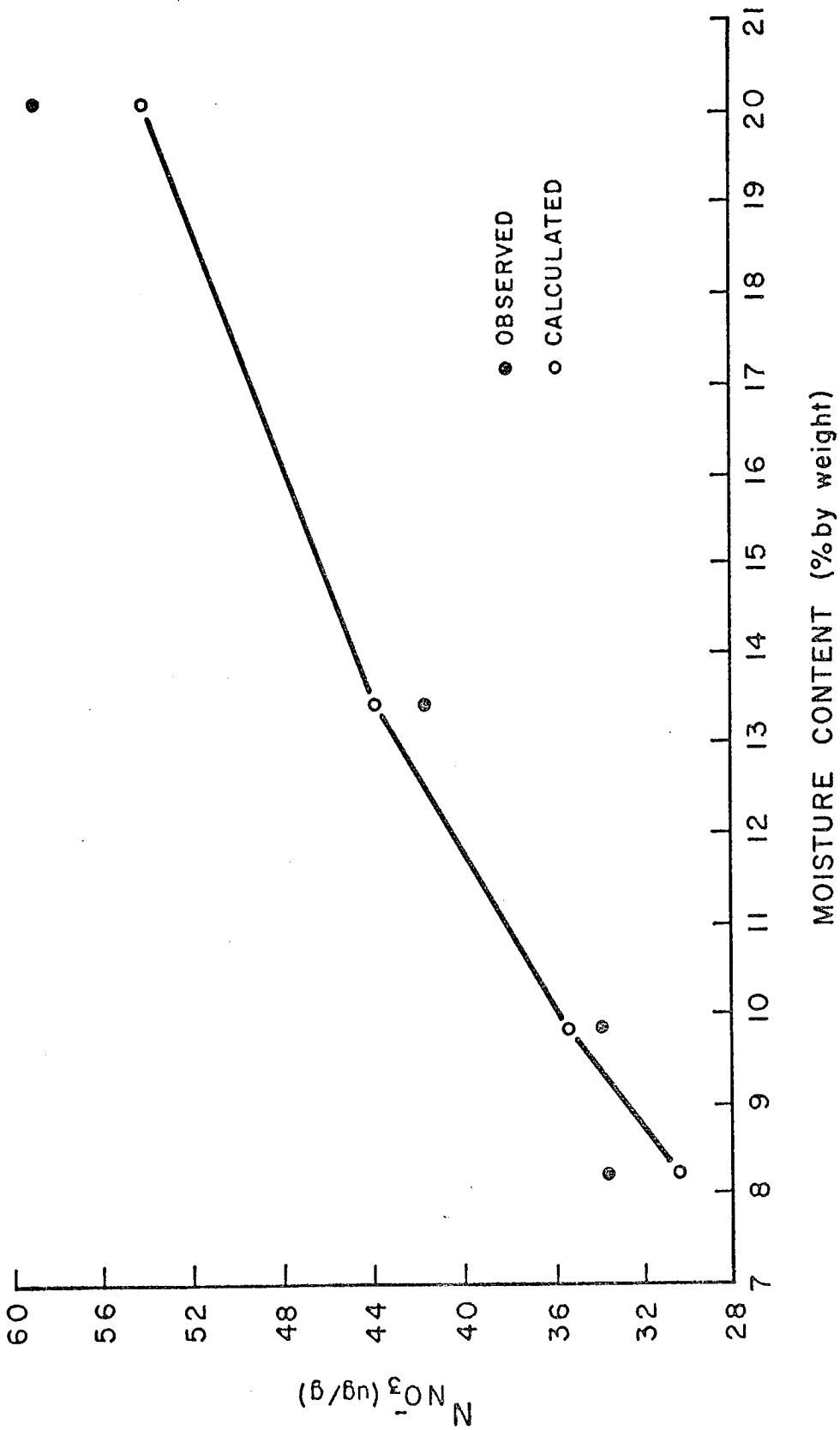


Figure 9. Calculated and Observed Rate Data for Gardena Soil at Various Moistures after 20 Days Incubation.

- (1966), see Table 2, and from data on soils with similar chemical properties. A summary of these estimates appears in Table 19.
6. The saturation constant for $N_{\text{NH}_4^+}$ was set equal to 5.0 ppm for the Parshall soil and 1.2 ppm (McLaren, 1970) for the Gardena soil. The 5.0 value was based on a regression study of measured activation energy (ΔE_m) versus μ at various assumed saturation levels for $N_{\text{NH}_4^+}$. The results of this study appear in Tables 20 and 21.
 7. Reichman et al. (1966) listed initial pH and pH values for the two soils after 20 days incubation at 0.2 bar suction. Other needed pH values were estimated from these values plus the assumption that pH changes were proportional to the reaction rate.

Table 19. Estimated Soil Extract Analyses Used in Verification of Nitrification Model

Parameter	Parshall	Gardena
Composition of Saturation Extract	meq/L	meq/L
CA ⁺⁺	1.90	3.61
Mg ⁺⁺	1.58	3.01
Na ⁺	0.84	1.60
HCO ₃ ⁻	1.82	3.47
CO ₃ ⁼	0.00	0.00
Cl ⁻	0.61	1.16
SO ₄ ⁼	1.46	2.79

Table 20. Statistical Data for $N_{NH_4}^+$ Saturation Values
in Parshall Soil

Saturation Value ($\mu\text{g } N_{NH_4}^+/\text{g soil}$)	R	s_y	s_b	F ratio
15.0	0.00361	0.542	23.3	0.001
10.0	0.178	0.346	14.9	0.329
8.0	0.358	0.240	10.3	1.21
5.0	0.756	0.155	6.67	13.3
4.0	0.684	0.468	8.97	8.78
3.0	0.626	0.268	11.5	6.45
2.0	0.626	0.268	11.5	6.45
1.0	0.626	0.268	11.5	6.45

Table 21. Statistical Data for $N_{NH_4}^+$ Saturation Values in Gardena Soil

Saturation Value ($\mu\text{g } N_{NH_4}^+/\text{g soil}$)	R	s_y	s_b	F ratio
15.0	0.00730	0.454	81.9	0.001
10.0	0.221	0.253	45.7	0.512
8.0	0.321	0.174	31.5	1.15
5.0	0.465	0.113	20.5	2.76
4.0	0.465	0.113	20.5	2.76
3.0	0.465	0.113	20.5	2.76
2.0	0.465	0.113	20.5	2.76
1.0	0.465	0.113	20.5	2.76

SUMMARY AND CONCLUSIONS

The objective of this study was the development of a transition state model to predict nitrification (nitrate formation) or ($\text{NH}_4^+ \rightarrow \text{NO}_3^-$) in soil-water systems.

An incubation study involving two soils provided rate data as a function of temperature, moisture content, pH, and $\text{N}_{\text{NH}_4^+}$ concentration. The assumption was made that the O_2 concentration remained above the saturation level and could be treated as a constant in the equations. Application of this data confirmed observations of other researchers that $\text{N}_{\text{NH}_4^+}$ oxidation is zero order with respect to $\text{N}_{\text{NH}_4^+}$ concentrations above a saturation level of about 1.0 to 5.0 ppm.

A computer model was tested to determine its ability to describe NH_4^+ exchange in these same soils. This model gave satisfactory predictions below about 20 to 40 percent moisture but needs improvement at higher moistures. The model was used to compute exchangeable NH_4^+ concentrations in this study since the moisture contents were relatively low.

A method was developed to compute soil pH values as a function of moisture content. An existing semi-empirical relationship was modified to include H^+ . The assumption was made that the slope in the relationship remains relatively

constant, but the intercept value shifts when H^+ is added to the soil-water system. Data pairing of calculated and observed pH values yielded correlation coefficients of 0.987 and 0.980 for the Panoche and desert soils, respectively.

The incubation data were used to attempt to learn something about the structure of the activated complex in NH_4^+ oxidation to NO_2^- . The conclusion was made that the complex or active part of the complex has a structure closer to NH_2OH or NH_4^+ than NO_2^- . Also, the equation form for the equilibrium between NH_4^+ and O_2 and the activated complex was investigated. The form was found to differ from the stoichiometric reaction between NH_4^+ and O_2 to form NH_2OH .

The model developed included NH_2OH as the activated complex and equation (74) as being representative of the equilibrium between the reactants and activated complex. A theoretical linear relationship between the measured activation energy and ionic strength was included in the model. The slope and intercept in this expression were calculated from experimental data for each soil. The linearity was found to be independent of soil, but microbial population sizes and other variations probably account for the different intercepts and slopes, respectively, encountered experimentally.

The model was applied to the Panoche and desert soils and yielded an R value of 0.956 for data pairing of 51 observed and calculated rates. Additional verification of the model was obtained by application to two soils from the Northern Great Plains. Data pairing of observed and calculated rate data showed R values of 0.944 and 0.940 for the Parshall and Gardena soils, respectively.

The model was programmed in FORTRAN IV computer language. This allowed the computations to be done easily and provided a simple means of connecting this model to existing or future simulation models. The nitrification rate predictions from the model should have application in optimization research, environmental impact studies, and soil fertility and plant nutrition.

APPENDIX A

COMPUTER LISTING OF RATE SUBROUTINE

SUBROUTINE NITR(ANH4,TEMP,AMOIS,UU,CA,RATE)

C-----THIS SUBROUTINE COMPUTES NITRIFICATION RATES BASED ON
C-----A TRANSITION STATE PHYSICO-CHEMICAL MODEL

C-----SLOPE,AINT, AND DELTAE1(U) MUST BE SPECIFIED FOR EACH
C-----SOIL

DIMENSION VTHA(8)

REAL K ,KD

COMMON/A/ H,K,PI, SORTPI

DATA (KD=3.0E-3), (V=1.E-18)

DATA (H=6.625E-27), (K=1.380E-16), (PI=3.142), (SORTPI=1.
1773)

DATA (RTA=7.47), (RTO=2.07), (DOO=8.138E-12), (DOA=8.138E
1-12)

DATA (VTO=2.23E3), (VT1A=6.051E3), (VT2A=4.299E3), (VT3A=
11.933E3)

DATA (VT4A=1.883E3), (VT5A=9.601E2), (OM=5.312E-23), (AM=
12.988E-23)

DATA (VTHA(1)=3.4E-4), (VTHA(2)=4.4E-4), (VTHA(3)=5.5E-4
1), (VTHA(4)=

16.4E-4), (VTHA(5)=6.8E-4), (VTHA(6)=7.2E-4), (VTHA(7)=8.4
1E-4), (VTHA(8)=8.7E-4)

C-----THESE CONSTANTS MUST BE SPECIFIED FOR EACH SOIL
DATA(SLOPE=-1.63), (AINT=4.460)

C-----FUNCTION FOR Q VIBRATIONAL
QVIBP(T,VT) =EXP(-VT/(2.*T))/(1.-EXP(-VT/T))

C-----FUNCTION FOR Q ROTATIONAL DIATOMIC MOLECULE
QROTD(T,SYM,RT) = T/(SYM*RT)

C-----FUNCTION FOR DERYE-HUCKEL ACTIVITY COEF
ACT(U) = 1./((10.**(+0.509*U/(1.0 + 1.00*U)))

C-----FUNCTION FOR ACTIVATION ENERGY AS A FUNCTION OF IONIC
C-----STRENGTH

C-----THIS FUNCTION MUST BE SPECIFIED FOR EACH SOIL
DELTAE1(U) = (40.70 + 0.6495*U)/1.439E13

C-----BEGIN CALCULATIONS

C-----CALL SUBROUTINE TO COMPUTE PH AT FIELD MOISTURE
CALL PHCALC(CA,AMOIS,SLOPE,AINT,PH)

```

C-----COMPUTE VIBRATIONAL TEMPERATURES FOR NH2OH
      DO 3 I=1,8
3      VTHA(I) = 3.0E10/VTHA(I)*H/K

C-----SET UPPER LIMIT FOR EXCHANGEABLE NH4 CONCENTRATION
      IF(CNH4 .GT.1.) CNH4 = 1.0

      CONVERT = 0.4976E12/AMOIS
      CTEMP = TEMP
      T = TEMP + 273.
      O2C = PPMO2(CTEMP)

C-----SET UPPER LIMIT FOR OXYGEN CONCENTRATION
      O2C = 0.25

C-----COMPUTE Q VIBRATIONAL FOR HYDROXYLAMINE
      QVIBHA = 1.0
      DO 2 I=1,8
2      QVIBHA = QVIBHA * QVIBP(T,VTHA(I))

C-----CONVERT UNITS TO NUMBER OF MOLECULES/ UNIT VOLUME
      CH = 10.**(-PH)*6.02E23/ACT(SQRT(UU))
      CNH4 = CNH4*4.30E16/AMOIS
      O2C = O2C*1.881E16

C-----COMPUTE Q TOTAL FOR OXYGEN
8      QO2 = QTRAN(T,V ,OM) * QPOTD(T,2.,RTO) * QVIBP(T,VT0)

C-----COMPUTE Q VIBRATIONAL FOR NH4
      QVIBA = QVIBP(T,VT1A)*QVIBP(T,VT2A)**4 * QVIBP(T,VT3A)
      1*QVIBP(T,VT4A)**2 * QVIBP(T,VT5A)

C-----COMPUTE TOTAL Q FOR NH4
      QNH4 = QTRAN(T,V ,AM) * QPOTP(T,12.,RTA,RTA,RTA) *QVIB
      1A

C-----COMPUTE TOTAL Q FOR HYDROGEN
      QH = QTRAN(T,V,1.66E-24)

C-----COMPUTE TOTAL Q FOR ACTIVATED COMPLEX(NH2OH)
      QHA=QTRAN(T,V,OM*1.03)*QPOTP(T,3.,RTA,RTA,RTO)*QVIBH
      1A

C-----COMPUTE DELTA E
      DELE = DELTAE1(UU)

C-----COMPUTE PART OF RATE FUNCTION
      X = EXP(-DELE/(K*T))*QHA

```

```

C-----CALL SUBROUTINE TO COMBINE PARTITION FUNCTIONS AND
C-----CONCENTRATIONS
      CALL COMP(V,QH,CNH4,O2C,QNH4,QO2,CH,T,SUB)

C-----COMPUTE RATE
      RATE = X*SUB

C-----CONVERT UNITS ON RATE TO UG/G SOIL/DAY
      RATE = RATE/CONVERT

C-----RETURN TO SUBROUTINE TRNSFM OR CALLING ROUTINE
      RETURN
      END
      FUNCTION QROTP(T,SYM,THA,THB,THC)

C-----THIS FUNCTION COMPUTES Q ROTATIONAL FOR A POLYATOMIC
C-----MOLECULE
      COMMON/A/ H,K,PI,SQRTPI
      QROTP = SQRTPI / SYM*SQRT(T**3/(THA*THB*THC))
      RETURN
      END
      FUNCTION QTRAN(T,V,M)

C-----THIS FUNCTION COMPUTES Q TRANSLATIONAL
      REAL K,M
      COMMON/A/ H,K,PI,SQRTPI
      QTRAN = V*(SQRT(6.28*M*K*T/(H**2)))**3
      RETURN
      END
      SUBROUTINE COMP(V,QH,CNH4,O2C,QNH4,QO2,CH,T,SUB)

C-----THIS SUBROUTINE COMBINES PARTITION FUNCTIONS AND CON-
C-----CENTRATIONS

      COMMON/A/ H,K,PI,SQRTPI

      REAL K

C-----BEGIN CALCULATIONS
      PART1 = K*T/(V*H)
      PART2 = (QH/V) * CNH4**2 * O2C
      PART3 = (QNH4/V)**2*(QO2/V) * CH
      SUB = PART1*PART2/PART3

C-----RETURN TO SUBROUTINE NITR
      RETURN
      END
      SUBROUTINE PHCALC(CA,AMOIS,SLOPE,AINT,PH)
C-----THIS SUBROUTINE COMPUTES PH AS A FUNCTION OF MOISTURE

```

```
C-----CONTENT
      REAL KDP,KP,KSP,K3

      DATA(KSP=5.012E-9),(K3=5.012E-11)

C-----BEGIN CALCULATIONS
      AMOIS = AMOIS*100.
      KP = 10.**(SLOPE*ALOG10(AMOIS) - AINT)
      KDP = KP*K3**2/KSP**2
      H = SQRT(KDP*CA)
      PH = -ALOG10(H)

C-----RETURN TO SUBROUTINE NITR
      RETURN
      END
```

APPENDIX B
COMPUTER LISTING OF GENERAL
COMPUTATIONAL PROGRAM

PROGRAM RATE(INPUT,OUTPUT,TAPE1=INPUT,PUNCH)

DIMENSION TEMP(99),O2C(99),CNH4(99),RATE(99),PH(99),CH
1(99),VTHA(9)
1,UU(99),AMOIS(99),RNH4(99),CONVERT(99),OHC(99),ORS(99)
1,CA(99)
REAL K,KD

COMMON/A/ H,K,PI,SQRTPI

DATA (KD=3.0E-3),(V=1.E-18)
DATA (H=6.625E-27),(K=1.380E-16),(PI=3.142),(SQRTPI=1.
1773)
DATA (RTA=7.47),(RTO=2.07),(DOO=8.138E-12),(DOA=8.138E
1-12)
DATA (VTO=2.23E3),(VT1A=6.051E3),(VT2A=4.299E3),(VT3A=
11.933E3)
DATA (VT4A=1.883E3),(VT5A=9.601E2),(OM=5.312E-23),(AM=
12.988E-23)
DATA (VTHA(1)=3.4E-4),(VTHA(2)=4.4E-4),(VTHA(3)=5.5E-4
1),(VTHA(4)=6.4E-4),(VTHA(5)=6.8E-4),(VTHA(6)=7.2E-4),(
1VTHA(7)=8.4E-4),(VTHA(8)=8.7E-4),(VTHA(9)=10.0E-4)
DATA(OC = 0.132)

C-----FUNCTION FOR Q VIBRATIONAL
QVIBP(T,VT) = EXP(-VT/(2.*T))/(1.-EXP(-VT/T))

C-----FUNCTION FOR Q ROTATIONAL DIATOMIC MOLECULE
QROTD(T,SYM,RT) = T/(SYM*RT)

C-----FUNCTION FOR DERBYE-HUCKEL ACTIVITY COEF
ACT(U) = 1./((10.**(+0.509*U/(1.0 + 1.00*U)))

C-----FUNCTION FOR O2 CONCENTRATION IN WATER AS A FUNCTION
C-----OF TEMPERATURE
PPMO2(T) = 14.619 - 0.40396*T + 8.3996E-3*T**2 - 8.991
15E-5*T**3

C-----FUNCTIONS FOR DELTA E AS A FUNCTION OF IONIC STRENGTH
DELTAE1(U) = (49.390 + 29.262*U)/1.439E13
DELTAE2(U) = (50.554 + 4.4562*U)/1.439E13

C-----BEGIN CALCULATIONS
III = 0
DO 3 I=1,8
3 VTHA(I) = 3.0E10/VTHA(I)*H/K
IPUNM = 1

C-----READ SLOPE AND MOISTURE AT WHICH PH WAS DETERMINED

```

600  READ 100, SLOPE, AMOIS
      DELE = 0.0
      SAVE = 0.0
      ITEST = 1
      J1=ICON=0
      PRINT 106
      DO 54 J=1,100

C-----READ RATE, NH4, R-NH4, PH, IONIC STRENGTH, AND TEMP.,
C-----MOISTURE CONTENT, CA ACTIVITY
      READ 100, RATE(J),CNH4(J),RNH4(J),PH(J),UU(J),TEMP(J),
      1AMOIS(J),ACA(J)

      IF(EOF,1)99,66
66   III = III + 1
      IF(RATE(J).EQ.0.0) GO TO 53
      J1=J1+1

C-----CALL SUBROUTINE TO COMPUTE PH
      CALL PHCALC(CA(J),PH(J),AMOIS(J),1,SLOPE,ACA,AMOIS)
      OBS(J) = RATE(J)
      CNH4(J) =          RNH4(J)
      IF(CNH4(J).GT.1.) CNH4(J) = 1.0

C-----SET CONVERSION FACTOR
      CONVERT(J) = 0.4976E12/AMOIS(J)
      CTEMP = TEMP(J) - 273.
      O2C(J) = 0.25
54   CONTINUE

C-----PRINT INPUT AND OTHER DATA
53   PRINT 105,(RATE(J),CNH4(J),O2C(J),TEMP(J),PH(J),J=1,J1
      1)
6    DO 1 J=1,J1
      T = TEMP(J)

C-----COMPUTE Q VIBRATIONAL FOR HYDROXYLAMINE
      QVIBHA = 1.0
      DO 2 I=1,8
2    QVIBHA = QVIBHA * QVIBP(T,VTHA(I))

C-----CONVERT UNITS TO NO. OF MOLECULES/UNIT VOLUME
      CH(J) = 1./10.**PH(J) * 6.02E20 /ACT(SQRT(UU(J))
      CNH4(J) = CNH4(J)*4.30E16/AMOIS(J)
      O2C(J) = O2C(J)*1.831E16
      RATE(J) = RATE(J) * CONVERT(J)
      OHC(J) = 1.E-14/(1./10.**PH(J))

C-----COMPUTE Q TOTAL FOR OXYGEN

```

```

8      QO2 = QTRAN(T,V ,OM) * QROTD(T,2.,RT0) * QVIBP(T,VT0)
C-----PARTITION FUNCTION FOR OH
      QOH=QTRAN(T,V,OM*.531)*QROTD(T,1.,RT0)*QVIRP(T,VT0)
C-----COMPUTE Q VIBRATIONAL FOR NH4
      QVIB4 = QVIBP(T,VT1A)*QVIBP(T,VT2A)**4 * QVIBP(T,VT3A)
      1*QVIRP(T,VT4A)**2*QVIBP(T,VT5A)
C-----COMPUTE TOTAL Q FOR NH4
      QNH4 = QTRAN(T,V ,AM) * QROTP(T,12.,RTA,RTA,RTA) *QVIB
      1A
C-----COMPUTE TOTAL Q FOR HYDROGEN
      QH = QTRAN(T,V,1.66E-24)
C-----COMPUTE TOTAL Q FOR HYDROXYLAMINE
      QHA=QTRAN(T,V,OM*1.03)*QROTP(T,3.,RTA,RTA,RT0)*QVIBH
      1A
C-----Q ROTATIONAL FOR N2O
      QRN20 = QROTD(T,1.,2.42)
C-----Q VIBRATIONAL FOR N2O
      QVN20 = QVIBP(T,850.)**2 * QVIBP(T,1840.)*QVIBP(T,320
      10.)
C-----Q TRANSLATIONAL FOR N2O
      QTRN20 = QTRAN(T,V,OM*1.38)
C-----TOTAL Q FOR N2O
      QN20 = QRN20*QVN20*QTRN20
      XXX = QHA
      IF(ITEST.EQ.1)700,701
700   IF(III.EQ.1) DELE = DELTAE1(UU(J))
      IF(III.EQ.2) DELE = DELTAE2(UU(J))
701   CONTINUE
      ICON = 1
      X = EXP(-DELE/(K*T))*XXX
C-----CALL SUBROUTINE TO COMBINE PARTITION FUNCTIONS
      CALL HYAMINE(V,QH,CNH4(J),O2C(J),QNH4,QO2,CH(J),RATE(J
      1),X,T,ICON,QOH,QHC(J))
      IF(ICON.EQ.1) GO TO 7
C-----COMPUTE DELTA E
      DELE = -(ALOG(X) -ALOG(XXX ))*(K*T) *1.439E13
      SAVE = SAVE + DELE
7     RATE(J) = RATE(J) / CONVERT(J)
      IF(ICON.EQ.1) DELE = DELE*1.439E13

```

SOION = UU(J)

C-----PRINT RESULTS

```
1 PRINT 101,OBS(J),RATE(J),TEMP(J),PH(J),SOION,DELE,QHA,
  10NH4,QO2
  IF(IPUNM.EQ.1) GO TO 600
  STOP
  IF(ICON.EQ.1) GO TO 600
```

C-----COMPUTE MEAN ACTIVATION ENERGY

```
DELE = SAVE/(J1*1.439E13)
ICON = 1
ACTIV = SAVE/J1
GO TO 6
99 STOP
```

```
100 FORMAT(8F10.0)
101 FORMAT(5X,6F10.4,3E15.3)
105 FORMAT(5F10.2)
106 FORMAT(1H1,*R(PPM/OA)*2X*NH4(PPM)*3X*O2(PPM)*3X
  1*TEMP(K)*8X*PH*)
109 FORMAT(5F10.4)
800 FORMAT(///1X*ACTIVATION ENERGY = *,F10.3)
END
FUNCTION QROTP(T,SYM,THA,THB,THC)
```

C-----THIS FUNCTION COMPUTES Q ROTATIONAL FOR POLYATOMIC
C-----MOLECULES

```
COMMON/A/ H,K,PI,SQRTPI

QROTP = SQRTPI / SYM*SQRT(T**3/(THA*THB*THC))
RETURN
END
FUNCTION QTRAN(T,V,M)
```

C-----THIS FUNCTION COMPUTES Q TRANSLATIONAL

```
REAL K,M

COMMON/A/ H,K,PI,SQRTPI

QTRAN = V*(SQRT(6.29*M*K*T/(H**2)))**3
RETURN
END
SUBROUTINE HYAMINE(V,QH,CNH4,O2C,QNH4,QO2,CH,RATE,X,T,
  1I,QOH,QHC)
```

C-----THIS SUBROUTINE COMBINES THE PARTITION FUNCTIONS

```
COMMON/A/ H,K,PI,SQRTPI
```

```
REAL K
```

```
C-----BEGIN CALCULATIONS
PART1 = K*T/(V*H)
PART2 = (QH/V) * CNH4**2 * O2C
PART3 = (QNH4/V)**2*(QO2/V) * CH
IF(I.EQ.1) GO TO 1
X = RATE/(PART1 * PART2/PART3)
RETURN
1 CONTINUE
RATE = X * (PART1 * PART2/PART3)
RETURN
END
SUBROUTINE PHCALC(CA,PH,AMOIS,IGOUNT,SLOPE,ACA,AAMOIS)
```

```
C-----THIS SUBROUTINE COMPUTES PH AS A FUNCTION OF MOISTURE
C-----CONTENT
```

```
REAL KDP,KP,KSP,K3
```

```
DATA(KSP=5.012E-9.,(K3=5.012E-11)
```

```
C-----BEGIN CALCULATIONS
BBMOIS = AAMOIS*100.
BMOIS = AMOIS*100.
KDP = (10.**(-PH))**2/ACA
KP = KDP*KSP**2/K3**2
AINT = SLOPE*ALOG10(BBMOIS) - ALOG10(KP)
1 KP = 10.**(SLOPE*ALOG10(BMOIS) - AINT)
KDP = KP*K3**2/KSP**2
H = SQRT(KDP*CA)
PH = -ALOG10(H)
RETURN
END
```

APPENDIX C

DATA COLLECTED IN INCUBATION STUDY

IDENT
 COL. 1-2 02 = PANOCHÉ SOIL
 01 = DESERT SOIL
 COL. 3-4 TIME IN DAYS
 COL. 5-6 TEMPERATURE IN DEGREES C

NH4 AMMONIUM N (UG/G SOIL)

NO3 NITRATE N + NITRITE N (UG/G SOIL)

MOIS MOISTURE CONTENT (G WATER/G AIR DRY SOIL)

IDENT	PH	NH4	NO3	MOIS
020015	8.32	132.7	19.9	.096
020015	8.31	127.4	19.6	.098
021415	8.20	128.9	74.2	.095
021415	8.32	81.6	92.1	.094
022815	8.20	92.4	154.7	.074
022815	8.20	76.4	176.7	.088
024615	8.26	22.9	301.1	.082
024615	8.30	49.6	235.3	.066
026015	8.35	53.4	226.1	.057
026015	8.30	23.1	285.7	.064
020015	8.40	127.3	16.6	.076
020015	8.38	129.9	13.2	.069
021415	8.25	148.6	24.3	.068
022815	8.25	143.0	29.1	.064
022815	8.25	150.1	34.3	.053
026015	8.50	136.8	33.2	.045
021415	8.26	122.2	13.4	.058
021415	8.28	155.2	9.2	.053
022815	8.30	146.2	11.6	.048
022815	8.30	154.7	14.8	.055
026015	8.50	147.7	15.6	.057
026015	8.49	146.2	15.6	.044
020025	8.28	175.6	11.4	.126
020025	8.33	177.8	13.7	.128
021125	8.10	92.9	85.3	.120
022525	8.09	10.7	266.1	.104
022525	8.08	4.0	282.9	.118
023925	8.29	4.6	381.1	.108
023925	8.27	4.5	376.3	.099
025325	8.48	2.3	369.7	.109
025325	8.41	4.5	370.9	.093
021125	8.25	133.4	9.4	.063
021125	8.25	132.4	8.4	.061
022525	8.30	120.8	10.4	.054
023925	8.41	141.5	12.3	.058

023925	8.48	157.2	13.0	.045
025325	8.65	116.9	12.3	.048
020025	8.24	172.0	12.0	.056
021125	8.30	134.5	11.7	.041
021125	8.25	129.1	11.4	.057
023925	8.40	150.0	13.1	.050
023925	8.41	145.6	12.3	.046
025325	8.60	123.4	12.4	.058
020035	8.32	174.1	13.0	.122
020035	8.25	161.8	13.1	.121
021135	8.25	149.4	23.6	.049
021135	8.28	148.1	21.6	.043
022535	8.30	108.6	16.2	.017
023935	8.40	146.4	15.9	.015
025335	8.50	129.6	16.2	.014
021135	8.30	151.0	17.1	.031
021135	8.30	155.8	17.8	.033
022535	8.28	118.0	8.8	.017
022535	8.35	117.5	13.3	.016
023935	8.45	157.3	11.3	.016
023935	8.43	154.1	11.5	.013
025335	8.58	139.5	10.6	.015
025335	8.55	152.9	7.2	.013
020035	8.36	172.1	11.7	.060
020035	8.38	175.2	13.1	.053
021135	8.26	158.5	17.9	.034
021135	8.31	162.7	15.2	.031
022535	8.35	119.5	11.9	.016
022535	8.30	115.0	7.6	.017
023935	8.35	157.9	10.4	.014
023935	8.43	157.3	9.2	.016
025335	8.58	151.5	13.4	.013
025335	8.60	143.7	10.1	.014
011415	6.63	159.3	117.1	.136
011415	6.70	163.2	114.8	.100
012815	6.45	165.9	112.1	.121
012815	6.60	151.9	131.7	.102
014615	6.33	157.5	130.1	.111
014615	6.38	165.4	122.5	.123
016015	6.41	142.3	142.1	.084
016015	6.43	144.3	140.0	.078
010015	6.85	92.7	101.4	.035
010015	6.85	174.8	112.7	.049
011415	6.84	159.2	126.8	.039
011415	6.90	159.1	125.9	.036
010015	6.80	156.3	112.6	.034
010015	6.65	155.4	116.7	.038
011415	6.84	146.2	121.2	.028
011415	6.72	153.5	114.1	.027
012815	6.75	141.4	135.5	.034

012815	6.65	151.4	124.3	.031
016015	6.65	148.7	137.5	.016
011125	6.40	112.3	111.6	.087
011125	6.60	111.1	117.3	.067
012525	6.68	147.2	117.0	.063
012525	6.48	143.6	146.9	.063
013925	6.55	142.6	147.0	.064
013925	6.45	134.2	165.3	.050
015325	6.55	132.8	165.4	.034
015325	6.40	135.9	160.9	.065
011125	6.58	114.9	83.6	.026
011125	6.82	120.8	92.0	.040
012525	6.80	117.8	106.7	.043
012525	6.70	147.0	135.0	.026
013925	6.80	148.5	161.4	.050
013925	6.89	145.1	132.9	.022
015325	6.72	140.5	134.6	.022
015325	6.80	164.4	137.3	.052
010025	6.95	123.4	82.9	.030
010025	6.95	145.5	69.1	.031
011125	6.62	155.9	95.7	.018
012525	6.95	89.6	100.1	.022
012525	6.95	162.5	93.5	.030
013925	7.00	171.2	103.2	.033
015325	7.12	167.0	111.0	.033
015325	7.08	163.0	107.3	.025
010035	6.69	114.5	103.5	.018
010035	6.75	112.0	110.3	.017
011135	6.42	150.2	133.2	.090
011135	6.37	148.4	138.6	.086
012535	6.78	142.4	131.5	.010
012535	6.69	139.8	147.9	.009
013935	6.69	138.6	153.6	.011
013935	6.78	137.8	139.1	.010
015335	6.55	137.5	146.9	.025
015335	6.62	140.5	141.0	.009
010035	6.70	95.0	87.2	.014
010035	6.95	118.0	92.6	.014
011135	6.69	152.9	106.1	.031
011135	6.80	151.1	110.6	.027
012535	6.80	141.6	109.6	.008
012535	6.78	150.8	129.6	.043
013935	6.82	143.0	109.5	.008
013935	6.80	152.5	116.7	.007
015335	6.75	140.5	114.2	.007
010035	6.65	108.9	120.5	.019
010035	6.40	109.8	103.6	.016
011135	6.39	141.1	155.2	.028
012535	6.52	133.4	155.8	.010
012535	6.50	146.7	150.4	.010

013935	6.80	144.4	146.5	.011
013935	6.60	145.0	135.1	.010
015335	6.60	129.7	158.8	.010
015335	6.45	148.1	140.5	.009

LITERATURE CITED

- Alexander, M. (1961) Introduction to soil microbiology. John Wiley and Sons, Inc., New York.
- Amis, E. S. (1949) Kinetics of chemical change in solution. The Macmillan Company, New York.
- Beesley, R. M. (1914) Experiments on the rate of nitrification. J. Chem. Soc. (London). 105:1014-1024.
- Boon, B. and Laudelout, H. (1962) Kinetics of nitrite oxidation by Nitrobacter winogradskyi. Biochem. J. 85:440.
- Broadbent, F. E., Tyler, K. B., and Hill, G. N. (1957) Nitrification of ammoniacal fertilizers in some California soils. Hilgardia. 27:247-267.
- Brown, E., Skougstad, M. W., and Fishman, M. J. (1970) Techniques of water-resources investigations of the United States geological survey: Methods for collection and analysis of water samples for dissolved minerals and gases. United States Government Printing Office, Washington, D.C., pp. 152-154.
- Campbell, N. E. R. and Lees, H. (1967) The nitrogen cycle. In soil biochemistry, McLaren, A. D. and Peterson, G. H., Ed. Marcel Dekker, Inc., New York. pp. 194-215.
- Caster, A. B., Martin, W. P., and Buehrer, T. F. (1942) Threshold pH values for the nitrification of ammonia in desert soils. Soil Sci. Soc. Amer. Proc. 7:223-228.
- Corbet, A. S. (1935) The formation of hyponitrous acid as an intermediate compound in the biological or photochemical oxidation of ammonia to nitrous acid. II. Microbial oxidation. Biochem. J. 29:1086-1096.
- Downing, A. L., Painter, H. A., and Knowles, G. (1964) Nitrification in the activated sludge process. J. Inst. Sew. Purif. No. 130.
- Dutt, G. R., Shaffer, M. J., and Moore, W. J. (1972) Computer simulation model of dynamic bio-physicochemical processes in soils. Ariz. Agr. Exp. Sta. Tech. Bul. No. 196.

- Frankland, P. F. and Frankland, G. (1890) The nitrifying process and its specific ferment. Trans. Roy. Soc. (London). B181:107.
- Fraps, G. S. and Sturges, A. J. (1939) Effect of phosphates on nitrifying capacity of soils. Soil Sci. 47:115-121.
- Fuller, W. H., Martin, W. P., and McGeorge, W. T. (1950) Behavior of nitrogenous fertilizers in alkaline calcareous soils: II. Field experiments with organic and inorganic nitrogenous compounds. Ariz. Agr. Exp. Sta. Tech. Bul. No. 121.
- Garrels, R. M. and Christ, C. L. (1965) Solutions, minerals, and equilibria. Harper and Row, New York.
- Greenwood, D. J. (1962) Nitrification and nitrate dissimilation in soil: II. Effect of oxygen concentration. Plant and soil. 17:378.
- Greenwood, D. J. (1968) Microbial metabolism. In the ecology of soil bacteria, Gray, T. R. G. and Parkinson, D., Ed. Liverpool University Press. p. 138.
- Griffin, D. M. (1963) Soil moisture and the ecology of soil fungi. Biol. Rev. 38:141-166.
- Harris, G. M. (1966) Chemical kinetics. D. C. Heath and Company, Boston.
- Hill, T. L. (1960) An introduction to statistical thermodynamics. Addison-Wesley Publishing Company, Inc., Reading, Mass.
- Hofman, T., and Lees, H. (1953) The biochemistry of the nitrifying organisms: 4. Biochem. J. 54:579-583.
- Johnson, D. D. and Guenzi, W. D. (1963) Influence of salts on ammonium oxidation and carbon dioxide evolution from soil. Soil Sci. Soc. Amer. Proc. 27:663-666.
- Jolly, W. L. (1964) Inorganic chemistry of nitrogen. W. A. Benjamin, Inc. New York.
- Justice, J. K. and Smith, R. L. (1962) Nitrification of ammonium sulfate in a calcareous soil as influenced by combinations of moisture, temperature, and levels of added nitrogen. Soil Sci. Soc. Amer. Proc. 26:246-250.
- Keeney, D. R. and Bremner, J. M. (1969) Determination of soil cation exchange capacity by a simple semimicro technique. Soil Sci. 107:334-336.

- Kluyver, A. J. and Donker, H. J. L. (1925) Catalytic transference of hydrogen as the basis of dissimilation processes. Proc. Acad. Sci. (Amsterdam). 28:605-618.
- Knowles, G., Downing, A. L., and Barrett, M. J. (1965) Determination of kinetic constants for nitrifying bacteria in mixed culture, with the aid of an electronic computer. J. gen. Microbiol. 38:263-278.
- Laidler, K. J. (1963) Reaction kinetics. Pergamon Press, New York.
- Laudelot, H. and van Tichelen, L. (1960) Kinetics of the nitrite oxidation by Nitrobacter winogradskyi. J. Bacteriol. 79:39-42.
- Lees, H. and Quastel, J. H. (1946) Kinetics of, and the effects of poisons on, soil nitrification, as studies by a soil perfusion technique. Biochem. J. 40:803-828.
- Longmuir, I. (1954) Respiration rate of bacteria as a function of oxygen concentration. Biochem. J. 57:81-87.
- Macauley, B. J. and Griffin, D. M. (1969) Effects of carbon dioxide and oxygen on the activity of some soil fungi. Trans. Brit. Mycol. Soc. 53:53-62.
- McIntosh, T. H. and Frederick, L. R. (1958) Distribution and nitrification of anhydrous ammonia in a Nicollet sandy clay loam. Soil Sci. Amer. Proc. 22:402-405.
- McLaren, A. D. (1970) Temporal and vectorial reactions of nitrogen in soil: A review. Can. J. Soil Sci. 50:97-109.
- McLaren, A. D. (1971) Kinetics of nitrification in soil: Growth of the nitrifiers. Soil Sci. Soc. Amer. Proc. 35:91-95.
- Meites, L. (1963) Handbook of analytical chemistry. McGraw-Hill Book Company, New York. pp. 3-204 - 3-205.
- Meyerhof, O. (1916) Untersuchungen über den atmungsvorgang nitrifizierenden bakterien: I. Die atmung des nitratbildners. Pflüg. Arch. ges. Physiol. 164:353-427.
- Miller, R. D. and Johnson, D. D. (1964) The effect of soil moisture tension on carbon dioxide evolution, nitrification, and nitrogen mineralization. Soil Sci. Soc. Amer. Proc. 28:644-647.
- Miyake, K. (1916) On the nature of ammonification and nitrification. Soil Sci. 2:481-492.

- Nicholus, D. J. D. and Jones, O. T. G. (1960) Oxidation of hydroxylamine in cell-free extracts of Nitrosomonas europaea, *Nature*. 185:512-514.
- Parker, D. T. and Larson, W. F. (1962) Nitrification as affected by temperature and moisture content of mulched soils. *Soil Sci. Soc. Amer. Proc.* 26:238-242.
- Pikovskaya, R. (1940) The activity of nitrifying bacteria of various soils. *Milrobiol. Zh.* 7:189-206.
- Pulley, H. C. and Greaves, J. D. (1932) An application of the autocatalytic growth curve to microbial metabolism. *J. Bact.* 24:145-168.
- Quastel, J. H. and Scholefield, P. G. (1951) Biochemistry of nitrification in soil. *Bact. Rev.* 15:1-53.
- Reichman, G. A., Grunes, D. L., and Viets, Jr., F. G. (1966) Effect of soil moisture on ammonification and nitrification in two northern plains soils. *Soil Sci. Soc. Amer. Proc.* 30:363-366.
- Robinson, J. B. D. (1957) The critical Relationship between soil moisture content in the region of the wilting point and the mineralization of natural soil nitrogen. *J. Agr. Sci.* 49:100-105.
- Sabey, B. R., Frederick, L. R., and Bartholomew, W. V. (1969) The formation of nitrate from ammonium nitrogen in soils: IV. Use of the delay and maximum rate phases for making quantitative predictions. *Soil Sci. Soc. Amer. Proc.* 33:276-278.
- Sadtler Research Laboratories (1967) Standard Spectra. Sadtler Research Laboratories, Inc., Philadelphia.
- Schloessing, J. H., and Muntz, C. A. (1877) Sur la nitrification par les ferments organises. *C. R. Acad. Sci. (Paris)* 8:301.
- Shaffer, M. J. (1970) Prediction of nitrogen transformations in alkaline soils. M.S. Thesis, The University of Arizona.
- Shaffer, M. J., Dutt, G. R. and Moore, W. J. (1969) Predicting changes in nitrogenous compounds in soil-water systems. Collected Papers Regarding Nitrates in Agricultural Waste Water. United States Government Printing Office, Washington, D.C. pp. 15-28.

- Stevens, B. (1970) Chemical Kinetics. Chapman and Hall Ltd. and Science Paperbacks, London.
- Stevens, F. L. and Withers, W. A. (1909) Studies in soil bacteriology: I. Nitrification in soils and in solutions. Cent. Bakt. II. 23:355-373.
- Stojanovic, B. J. and Alexander, M. (1958) Effect of inorganic nitrogen on nitrification. Soil Sci. 86:208-215.
- Warington, R. (1891) On nitrification. J. Chem. Soc. 59:484.
- Winogradsky, S. (1890) Recherches sur les organismes de la nitrification. Ann. Inst. Pasteur. 4:213-771.
- Yoshida, T. and Alexander, M. (1964) Hydroxylamine formation by Nitrosomonas europaea. Can. J. Microbiol. 10:923-926.
- Yoshida, T. and Alexander, M. (1971) Hydroxylamine oxidation by Nitrosomonas europaea. Soil Sci. 111:307-312.